



HAL
open science

RavA-ViaA antibiotic response is linked to Cpx and Zra2 envelope stress systems in *Vibrio cholerae*

Evelyne Krin, André Carvalho, Manon Lang, Anamaria Babosan, Didier Mazel, Zeynep Baharoglu

► **To cite this version:**

Evelyne Krin, André Carvalho, Manon Lang, Anamaria Babosan, Didier Mazel, et al.. RavA-ViaA antibiotic response is linked to Cpx and Zra2 envelope stress systems in *Vibrio cholerae*. *Microbiology Spectrum*, In press, 10.1128/spectrum.01730-23 . pasteur-04260034

HAL Id: pasteur-04260034

<https://pasteur.hal.science/pasteur-04260034>

Submitted on 26 Oct 2023

HAL is a multi-disciplinary open access archive for the deposit and dissemination of scientific research documents, whether they are published or not. The documents may come from teaching and research institutions in France or abroad, or from public or private research centers.

L'archive ouverte pluridisciplinaire **HAL**, est destinée au dépôt et à la diffusion de documents scientifiques de niveau recherche, publiés ou non, émanant des établissements d'enseignement et de recherche français ou étrangers, des laboratoires publics ou privés.



Distributed under a Creative Commons Attribution 4.0 International License

RavA-ViaA antibiotic response is linked to Cpx and Zra2 envelope stress systems in *Vibrio cholerae*

Evelyne Krin* 1, André Carvalho* 1,2, Manon Lang 1,2, Anamaria Babosan 1, Didier Mazel** 1, Zeynep Baharoglu** 1

1 Institut Pasteur, Université Paris Cité, CNRS UMR3525, Unité Plasticité du Génome Bactérien, F-75015 Paris, France

2 Sorbonne Université, Collège doctoral, F-75005 Paris, France

* : equal contribution

** : co-corresponding authors didier.mazel@pasteur.fr and zeynep.baharoglu@pasteur.fr

Abstract

RavA-ViaA were reported to play a role in aminoglycoside sensitivity but the mechanisms remain elusive. Here, we performed competition and survival experiments to confirm that deletion of *ravA-viaA* increases tolerance of the Gram-negative pathogen *Vibrio cholerae* to low and high aminoglycoside concentrations, during aerobic growth. Using high throughput strategies in this species, we identify Cpx and Zra2 two-component systems as new partners of RavA-ViaA. We show that the aminoglycoside tolerance of Δ *ravvia* requires the presence of these membrane stress sensing two-component systems. We propose that deletion of the RavA-ViaA function facilitates the response aminoglycosides because of a pre-activated state of Cpx and Zra2 membrane stress response systems. We also find an impact of these genes on vancomycin resistance, and we show that simultaneous inactivation of *ravvia* function together with envelope stress response systems leads to outer membrane permeabilization. Vancomycin is mostly used for Gram-positive because of its low efficiency for crossing the Gram-negative outer membrane. Targeting of the *ravA-viaA* operon for inactivation could be a future strategy to allow uptake of vancomycin into multidrug resistant Gram-negative bacteria.

Importance

The RavA-ViaA complex was previously found to sensitize *Escherichia coli* to aminoglycosides in anaerobic conditions, but the mechanism is unknown. Aminoglycosides are antibiotics known for their high efficiency against Gram-negative bacteria. In order to elucidate how the expression of the RavA-ViaA genes increases bacterial susceptibility to aminoglycosides, we aimed at identifying partner functions necessary for increased tolerance in the absence of RavA-ViaA, in *V. cholerae*. We show that membrane stress response systems Cpx and Zra2 are required in the absence of *ravA-viaA*, for the tolerance to aminoglycosides and for outer membrane integrity. In the absence of these systems, the Δ *ravvia* strain's membrane become permeable to external agents such as the antibiotic vancomycin.

Introduction

Antibiotic resistance is a growing public health problem. Common resistance mechanisms developed by bacteria consist of limiting antibiotic entry, increasing efflux, degrading the antibiotic or mutating the target. Decreasing intracellular concentrations of antibiotics is one of the most frequent resistance strategies. The aminoglycoside (AG) class of antibiotics targets the ribosome, leading to mistranslation, protein misfolding and eventually cell death. AGs are highly efficient against Gram-negative bacteria [1]. They comprise kanamycin, tobramycin, gentamicin, neomycin, amikacin and

streptomycin and are commonly used worldwide. The currently accepted model for AG entry [2, 3] starts with the PMF-dependent [4-6] and respiration-dependent [7-9] entry of a small AG quantity, leading to mistranslation by the ribosome. Incorporation of mistranslated proteins would then lead to membrane damage and a subsequent second step AG uptake in large amounts [6, 10].

The *ravA-viaA* operon (formerly *yieMN*) was found to sensitize Gram-negative bacteria to the AGs [11], but the mechanism remains elusive. The presence of RavA-ViaA has been reported mostly in γ -proteobacteria. Notably, *ravA-viaA* were found in 37 out of 50 randomly chosen enterobacteria [12]. RavA (regulatory ATPase variant A) belongs to the class of P-loop AAA+ proteins, which hydrolyze ATP and are involved in diverse molecular processes such as protein degradation, assembly of membrane complexes, DNA repair, and others. ViaA (VWA interacting with AAA+ ATPase) carries a von Willebrand factor type A (VWA) domain and interacts with RavA and stimulates its ATPase activity [13]. Structural work revealed that RavA and ViaA interact with each other [13], and form a complex with a third partner, LdcI (or CadA) [12, 13], leading to a cage-like structure up to 1 MDa in size [14]. It was also shown that the RavA-ViaA complex interacts with phospholipids at the inner membrane [15].

The involvement of *ravA-viaA* genes in AG susceptibility was originally identified by independent approaches in different proteobacteria, *Escherichia coli* [11] and *Vibrio cholerae* [16]. In *E. coli*, overexpression of *ravA-viaA* sensitizes to gentamicin, and its deletion was shown to increase AG resistance [11, 17] but only in anaerobic conditions and low energy state [15, 18]. In *V. cholerae*, the *ravA-viaA* operon (VC_A0762-VC_A0763) is also involved in the response to low doses (below MIC, or sub-MIC) of AGs, this time in aerobic conditions. While studying the response of *V. cholerae* to sub-MIC tobramycin we have conducted a high throughput transposon insertion sequencing (TN-seq) screen [19, 20] where the most enriched insertions were detected in the VC_A0762 (*viaA*) and VC_A0763 (*ravA*) genes (respectively 60x and 30x enrichment), suggesting that inactivation of the operon confers a growth advantage in the presence of AGs in *V. cholerae*. This is consistent with our previous results showing that genotoxic stress induced by tobramycin is limited in the absence of this operon [16].

The PMF is involved in the first phase of AG uptake [21], while the second phase occurs in response to mistranslation (or through sugar transporters). PMF is produced by the activity of electron transfer chains in respiratory complexes, where Fe-S cluster are key actors. It was shown that Fe-S biogenesis and their fueling to respiratory complexes have a direct impact on AG uptake [22]. Previous studies reported that RavA and ViaA interact with Fe-S cluster biogenesis machineries and also with components of the major Fe-S cluster containing Nuo respiratory complex [11, 23], suggesting that RavA-ViaA could contribute to folding of the respiratory complex I. Therefore, it was proposed that RavA and ViaA sensitize *E. coli* to AGs by facilitating Fe-S targeting to complex I and as a consequence an increased level of PMF. Note that *E. coli* and *V. cholerae* are very dissimilar in respect to the respiration complexes, Fe-S biogenesis and oxidative stress response pathways. For instance, *V. cholerae* lacks the above mentioned Cyo/Nuo complex I, and lacks also the SUF Fe-S biogenesis system used under oxidative stress. RavA-ViaA complex, was thus proposed to allow AGs to accumulate inside the cells, presumably by enhancing their uptake of AGs [18].

In order to shed light into how these genes modulate bacterial susceptibility to AGs, it's important to understand in which conditions these genes are expressed, which bacterial functions are necessary for AG sensitization, and which bacterial processes are affected by these genes.

Here, we first extensively confirmed the RavA-ViaA dependent AG susceptibility and tolerance phenotypes in *V. cholerae*. Next, high throughput approaches identified the involvement of envelope stress responses in these phenotypes. TN-seq showed that inactivation of *cpxP* repressor, i.e. activation Cpx response, is beneficial in Δ *ravvia*. Cpx responds to conditions that cause misfolding of inner membrane (IM) and periplasmic proteins, and subsequent membrane defect (for review[24]). Cpx also down-regulates outer membrane proteins (OMPs). In parallel, transcriptomic data in Δ *ravvia* showed strong induction of VC_1314 and the VC_1315-VC_1316 operon which presents similarities with the Cpx and Zra two-component envelope stress response systems. In *E. coli*, ZraSR contributes to antibiotic resistance and is important for membrane integrity [25]. Δ *zra* has increased membrane

disruption during treatment with membrane targeting antibiotics. Zra chaperone activity is enhanced in the presence of zinc ions. In this case, zinc was proposed to be a marker of envelope stress perturbation where ZraPSR is a sentinel sensing and responding to zinc entry into the periplasm [26].

We find that the AG tolerance conferred by *ravA-viaA* deletion in *V. cholerae* requires the presence of the Cpx system and Zra-like system, which we propose to name *zraP2-zraS2-zraR2*. We further show for the first time that *ravA-viaA* deletion together with inactivation of Cpx or Zra2 envelope stress responses leads to outer membrane permeabilization and may confer vancomycin sensitivity to Gram-negative bacteria.

Results

ravvia* deletion decreases sub-MIC aminoglycoside susceptibility in *V. cholerae

In order to evaluate AG related roles of RavA-ViaA, we assessed the effect of *ravA-viaA* deletion (referred to as Δ *ravvia* below) and overexpression (chromosomal extra-copy, referred to as WT::*ravvia*OE+, where OE stands for overexpression). We first performed competitions against *V. cholerae* WT, in the absence and presence of sub-MIC doses of AGs: tobramycin (TOB) and gentamicin (GEN), and also of antibiotics from families other than AGs: chloramphenicol (CM) that targets translation and ciprofloxacin (CIP) that targets DNA replication.

Competition results show that (**Figure 1A**) (i) *V. cholerae* Δ *ravvia* has a growth advantage compared to WT during growth with AGs TOB and GEN (40 and 50 % MIC); (ii) *V. cholerae* WT::*ravvia*OE+ has a growth disadvantage compared to WT with TOB and GEN; (iii) no significant effect is observed in the presence of sub-MICs of tested antibiotics other than AGs. This suggests the specificity of the mechanism of action of RavA-ViaA to AGs, in *V. cholerae*. Note that the beneficial effect of Δ *ravvia* is observed here during aerobic growth, while in *E. coli*, it can only be observed in anaerobic conditions.

ravvia* deletion increases tolerance to high doses of aminoglycosides in *V. cholerae

Next, we tested the effect of *ravvia* deletion on resistance by measuring the minimal inhibitory concentration (MIC), and on survival to lethal treatment with AGs. The MIC of Δ *ravvia* seemed unchanged, or slightly increased compared to WT (1.2 to 1.5 μ g/ml instead of 1.2 μ g/ml) (**Table 1**). Single Δ *ravA* or Δ *viaA* show the same MIC as the deletion of the whole operon, as expected, since the two proteins form a complex. The *ravvia*OE+ mutant shows lower resistance (MIC at 0.75 μ g/ml) (**Table 1**).

For survival to lethal treatment, we tested the tolerance of the strains to 5x and 10x MIC TOB doses for 6 hours. Deletion of *ravvia* strongly increases survival to lethal TOB doses, when compared to the WT strain (**Figure 1B**). No effect is observed upon treatment with CIP, Trimethoprim and Carbenicillin (**Figure S1**). Treatment to TOB 5 μ g/ml during 3 hours shows that Δ *ravvia* is not affected by TOB during this treatment window (**Figure 1B**), but these cells still die upon longer treatment periods (6 hours) (**Figure 1B**), excluding any bacteriostatic action of AGs in Δ *ravvia* mutant. Thus, Δ *ravvia* is killed upon lethal AG treatment, even though at a much slower rate than the WT, which is the definition of a tolerant population [27].

The effect of *ravvia* is only partly due to differential aminoglycoside uptake

We tested whether RavA-ViaA complex impacts AG entry, using the AG neomycin coupled to the fluorophore Cy5 (Neo-cy5), as previously done [28-30]. Neo-cy5 is a fluorescent AG specifically designed for bacterial uptake studies retains the properties of AGs in terms of uptake, mode of action, and activity against Gram-negative bacteria [31]. In this assay, cell fluorescence is proportional to Neo-cy5 uptake. AG uptake increased in *ravvia*OE+ (**Figure 2A**), suggesting that RavA-viaA overexpression facilitates AG entry into the bacterial cell. Surprisingly, AG uptake is not decreased in *V. cholerae* Δ *ravvia* (**Figure 2A**). Since AG uptake depends on PMF, we tested the effect of Δ *ravvia* on PMF. We used Mitotracker assay [29, 32], based on a fluorescent dye which accumulates inside the cell in a PMF

dependent way. We observed increased PMF in *ravvia*OE+ strain (**Figure 2B**), strengthening the notion that increased AG entry of *ravvia*OE+ is due to increased PMF. Conversely, no significant decrease of PMF was detected in the AG tolerant Δ *ravvia* strain (**Figure 2B**), suggesting that the effect of *ravvia* on AG susceptibility may require additional explanation as simply PMF modulation. Moreover, as expected, *sdh* (succinate dehydrogenase) deletion increased fitness in AGs, because of a decrease in PMF [5]. Simultaneous deletion of *sdh* and *ravvia* shows an additive fitness advantage (**Figure 2C**), suggesting that the mechanisms of increased fitness of Δ *ravvia* in sub-MIC TOB is not through a common pathway with the Δ *sdh*-dependent PMF decrease.

High throughput approaches point to a role of membrane stress two-component systems in Δ *ravvia*

In order to further understand changes due to *ravvia* deletion and to search for potential partners of RavA-ViaA, we decided to adopt transcriptomic and TN-seq approaches (**Figure 3**). RNA-seq was performed on exponentially growing WT and Δ *ravvia*. Major changes in Δ *ravvia* compared to WT include more than 10-fold upregulation of sugar transporters, anaerobic respiration, consistent with recent study published by the Barras and Py laboratories [18] and [33], and the VC_1314-1315-1316 genes (**Table S1**).

The VC_1314 gene and the VC_1315-VC_1316 operon show 8- to 10-fold upregulation. VC_1315 presents 35 % sequence identity with *E. coli zraS* gene. The ZraP regulator and ZraSR two-component membrane stress response system is involved in antibiotic resistance [25]. VC_1315 also presents 29 % (and 21 %) sequence identity with the *V. cholerae* (and *E. coli*) *cpxA* gene. The periplasmic CpxP is the negative regulator of the envelope stress response CpxRA system [34]. VC_1316 presents 26 % sequence identity with the *E. coli cpxR* and 23 % with the *V. cholerae cpxR*. VC_1314 does not show any sequence similarity neither to *zraP*, nor to *cpxP*. In *E. coli*, The CpxP-CpxAR system and the ZraP-ZraRS systems, were proposed to be functional homologues [26]. We called VC_1314-1315-1316, the *zra-like* system below in this manuscript.

In parallel to the transcriptomic study, we applied our previously described comparative TN-seq approach [16, 19], to *V. cholerae* Δ *ravvia*, to search for genes that are important for survival in the presence of sub-MIC TOB, again in aerobic conditions. We sequenced mutant libraries before and after 16 generations without and with TOB at 50% of the MIC. After sequencing, comparative analysis of the number of detected gene inactivations between the two conditions, indicates whether a given gene is important for growth in the antibiotic (decreased number of reads), or whether its inactivation is beneficial (increased number of reads), or unchanged. **Tables S2, S3 and S4** show the exhaustive lists of at least 2-fold differentially detected genes with transposon insertions in WT and Δ *ravvia*, with and without TOB. Deletion of *ravvia* leads to changes in factors involved in carbon metabolism, iron and respiration, and membrane stress. We constructed deletion mutants in WT and Δ *ravvia* contexts and performed competition experiments (**Figure S2**) for 21 of these genes to validate TN-seq results and to identify factors necessary for AG tolerance of Δ *ravvia*. Competition results were mostly consistent with TN-seq data. Among identified factors, one, *cpxP*, has particularly caught our attention because its inactivation is beneficial in Δ *ravvia* (**Figure S2**), and because inactivation of *ravvia* in Δ *cpxP* does not cause an additional increase in fitness, suggesting that they may act in the same pathway. Note that unlike CpxP, the *E. coli* ZraP represses the expression of the *zraPSR* operon only when bound to zinc [26]. In the conditions of our TN-seq experiments in *V. cholerae*, there is no zinc supplementation, so if VC_1314 is a ZraP-like protein, it is not necessarily a repressor under the tested conditions. Upon envelope stress, *E. coli* Δ *zraP* shows increased membrane disruption [25]. At T0, we counted 1.4-fold less insertions in *zraP-like* (VC_1314) in Δ *ravvia*, than the WT, suggesting that in the absence of *ravvia*, ZraP function is more important. This is statistically significant ($padj= 7.3 \times 10^{-5}$) but below the 2-fold change threshold and that's why it does not appear in the TN-seq results tables. Because Cpx and Zra-like systems were identified both in TN-seq, and in RNA-seq, we decided to focus on the link between the AG tolerant phenotypes of Δ *ravvia* and envelope stress response through the Cpx and Zra-like systems.

Cpx and Zra-like system mediated envelope stress response systems are necessary for the fitness advantage of *Δravvia* during growth with sub-MIC AGs and AG tolerance

In order to assess the importance of the Cpx and the putative Zra-like systems in the response to AGs of *Δravvia*, we tested fitness and tolerance in competition and survival experiments in the absence of one or both of these systems. **Figure 4ABC** shows competition experiments with *cpx* and *zra-like* operons inactivation (**Figure S3** shows the same competitions with statistical significance compared to the WT strain). Inactivation of *cpx* alone does not affect fitness in TOB (**Figure 4A**) while inactivation of *zra-like* alone increases fitness in TOB (**Figure 4B**). The fitness advantage of *Δzra-like* depends on the presence of *cpx*, since deletion of *cpx* in *Δzra-like* suppresses its fitness advantage (**Figure 4C**). Strikingly, the deletion of *cpx* or *zra-like* in *Δravvia* leads to, respectively, loss or strong decrease of the fitness advantage of *Δravvia* in TOB (**Figure 4A and B**). The triple mutant *Δravvia Δcpx Δzra* shows a phenotype similar to the *Δravvia Δcpx* double mutant (**Figure 4C**). We performed additional competitions to ascertain the effect of deletion of *zra* in *Δravvia Δcpx*, this time by competing the triple *Δravvia Δcpx Δzra* with *Δravvia Δcpx*. We observe that deletion of *zra* has in fact an additional negative impact on the fitness of *Δravvia Δcpx* (**Figure 4D**). These results show that Cpx envelope stress response system is necessary for the enhanced tolerance of *Δravvia* to TOB, and that the Zra-like system also contributes significantly to this fitness advantage.

We next performed TOB tolerance tests using a concentration of 5x MIC for 3 hours (**Figure 4E**). Under these conditions, the survival of the single *Δzra-like* system mutant is slightly lower than WT, the survival of *Δcpx* is lower and both systems seem to be additive as the double mutant appears to show even lower tolerance than the single *Δcpx*. Strikingly, the high level of tolerance of *Δravvia* is completely lost upon deletion of *zra-like* and goes even lower than WT upon deletion of *cpx* and in the triple mutant. For unknown reasons, the decrease of tolerance is stronger in *Δzra-like Δcpx* than in *Δzra-like Δcpx Δravvia*, as if deletion of *zra-like* in *Δravvia Δcpx* was beneficial. In any case, the AG tolerance conferred by the deletion of *ravvia* necessitates the presence of both Cpx and Zra-like systems.

***Δravvia* related phenotypes are linked to extracellular zinc concentrations**

Since Cpx and Zra systems have previously been associated with metals such as iron and zinc, we next performed competition experiments in the presence of these metals. The presence of supplemented iron did not affect the fitness of the *Δravvia* derivatives in any condition (**Figure S4ABC**). Zinc supplementation (**Figure 5ABC**) restores fitness in TOB for the *Δravvia Δcpx* and *Δravvia Δcpx* double mutants but not for the triple mutant, suggesting that the effect of zinc in *Δravvia* is somehow linked to the Cpx and Zra-like systems, which may act in a redundant way.

Moreover, while zinc has no effect on the TOB tolerance phenotype of *Δravvia* or *Δravvia Δzra-like*, it restores high tolerance to the *Δravvia Δcpx* mutant (**Figure 5D**), which is consistent with the zinc-dependent increase of fitness of the *Δravvia Δcpx* mutant shown in **Figure 5C**. We wondered whether these genes could be regulated by zinc. We found that *cpx*, but not *zra*, mRNA levels are increased in the presence of zinc (**Figure 5E**). *Ravvia* expression from *Pravvia* promoter fused to *gfp* is also induced by zinc (**Figure 5F**). Overall, results indicate that the *Δravvia* mutant's AG tolerance is dependent on the Cpx and Zra-like systems, and that *ravvia* function is also somehow associated with the sensing of zinc levels.

***Δravvia* has a low ROS phenotype which depends on Cpx/Zra**

We have previously shown that sub-MIC TOB leads to reactive oxygen species (ROS) formation in *V. cholerae*, which induces the bacterial SOS stress response [35]. However $\Delta ravvia$ is not more resistant to H_2O_2 (not shown). Considering that $\Delta ravvia$ is more tolerant to TOB and that $\Delta ravvia$ fails to induce SOS response in presence of TOB [16], we hypothesized that these two observations could be explained by a diminished ROS formation in $\Delta ravvia$. We used the CellROX dye that, upon increased levels of ROS (O_2^- and $\bullet OH$), emits green fluorescence. We observed that lack of *ravvia* in *V. cholerae* leads to decreased ROS generation, both in the absence and presence of sub-MIC TOB (**Figure 6, MH and sub-MIC TOB**). We similarly observed that $\Delta ravvia$ produces decreased levels of ROS upon treatment with lethal doses of TOB (**Figure S5**).

We next tested whether the function of Cpx/Zra-like systems in $\Delta ravvia$ could be involved in the “low ROS” phenotype observed for $\Delta ravvia$. **Figure 6** shows that the deletions of either *cpx* or *zra-like* (or both) suppress this phenotype, meaning that both Zra-like and Cpx are involved in the low ROS phenotype of $\Delta ravvia$. This is consistent with the fact that both systems are also necessary for AG tolerant phenotype of $\Delta ravvia$. As a control, we also tested the double mutant $\Delta ravvia \Delta bcp$. Bcp is a thiol peroxidase responding to oxidative stress. We see no effect of *bcp* deletion on the low ROS phenotype of $\Delta ravvia$. In conclusion, $\Delta ravvia$ shows a low ROS phenotype, which is reversed upon inactivation of Cpx and Zra-like stress responses.

Simultaneous deletion of Cpx or Zra-like systems with $\Delta ravvia$ leads to outer membrane permeability

Since Cpx and Zra systems, have been known for their involvement in envelope stress response, we decided to test the effect of *ravvia* deletion mutant and derivatives on outer membrane permeability.

Vancomycin is an antibiotic targeting the synthesis of the peptidoglycan, but which cannot be used to treat gram-negative bacteria, because its large molecular weight prevents it from crossing the outer membrane (OM) through porins, and penetrate into the cell [36]. When the OM is damaged however, vancomycin uptake by gram negative bacteria is possible [37] [38]. We tested whether deletion of *ravvia* has an impact on vancomycin entry, by measuring the MICs of the different mutants. Our results show that single deletions of $\Delta ravvia$, Δcpx or $\Delta zra-like$ do not affect the MIC to vancomycin, while double deletions of $\Delta ravvia$ together with Δcpx or $\Delta zra-like$ or both decreases the MIC from $>256 \mu g/ml$ to about $64-100 \mu g/ml$ (**Figure 7A**), suggesting that simultaneous inactivation of *ravvia* function together with envelope stress response systems leads to OM damage or permeabilization.

Changes in OM permeability can be quantified using nitrocefin [39], a chromogenic probe which develops color (at 490 nm) upon entry into the periplasm, in the presence of β -lactamase. We thus measured permeability of $\Delta ravvia$ and $\Delta cpx/\Delta zra-like$ derivatives transformed with the low-copy pSC101 plasmid carrying the *bla* gene. Again, results show that neither single deletions of $\Delta ravvia$, Δcpx or $\Delta zra-like$, nor the double $\Delta cpx \Delta zra-like$ deletion affect nitrocefin entry, while double deletions of $\Delta ravvia$ together with Δcpx or $\Delta zra-like$ or both, strongly increases it, consistent with increased OM permeability (**Figure 7B**).

Since AGs also are also expected to cross the cell envelope with higher efficacy with increased OM permeability, we checked whether AG uptake is increased in $\Delta ravvia \Delta cpx$ or $\Delta ravvia \Delta zra-like$ or the triple mutant (**Figure 7C**). Consistent with vancomycin and nitrocefin entry results, neo-cy5 uptake is also increased in $\Delta ravvia \Delta cpx$, $\Delta ravvia \Delta zra-like$, but not in single mutants or the $\Delta cpx \Delta zra-like$ mutant. Altogether, these results point to increased outer membrane permeability when either Cpx or Zra-like system is inactivated in $\Delta ravvia$.

Discussion

This study presents the first evidence of a link between RavA-ViaA function and the response to envelope stress. In fact, we identify the Cpx and a Zra-like two-component systems to be involved in the increased tolerance of *V. cholerae* *Δravvia* to AGs. Since Cpx and Zra systems are known to respond to protein misfolding at the periplasm, one can speculate that inactivation of *ravvia* could generate an increase in misfolded periplasmic proteins.

In *E. coli*, *Δcpx* mutants show alterations in conjugational plasmid transfer, transport, ability to grow on some carbon sources and resistance to AGs. More generally, the *E. coli* Cpx transcriptome impacts inner membrane associated processes such protein secretion, and other processes like iron homeostasis, translation, and interestingly, ribosome protection factors *raiA* and *rmf* [34]. Cpx also negatively regulates respiration, energy, and TCA cycle genes. In *V. cholerae*, Cpx senses and responds to low iron, and induces iron transporters and efflux pumps [40]. Disruption of the OM and accumulation of misfolded proteins in the periplasm were shown to induce the Cpx regulon [41-43]. The fact that our TNseq data also identified the *tat* operon as important for the growth advantage of *Δravvia* in TOB also supports the existence of a so far unknown link between RavA-ViaA and misfolded proteins in the periplasm. Cpx activity is regulated by successive phosphorylations (except for *cpxP*): envelope stress leads to phosphorylation and activation of CpxA, which phosphorylates and activates CpxR [44]. Envelope stress in parallel inactivates the repressor CpxP, because CpxP binds misfolded membrane proteins and is thus titrated away from CpxA. Thus, the Cpx activity is not solely regulated by activation of the promoter.

Such protein misfolding at the periplasm can happen during AG treatment, and Cpx was in fact previously linked to AG resistance [7, 45]. Interestingly, Cpx was also shown to induce the heat-shock sigma factor RpoH in the presence of the AG gentamicin, indicating that the effect AG gentamicin at the membrane is sufficient to trigger the response to misfolded IM protein stress by Cpx [46]. *ΔcpxR* is more susceptible to AGs in *E. coli* [47], and in *Salmonella* independently of efflux pumps [48], and also independently of oxygen consumption or PMF [47], but involves altered protein composition at the membrane [49]. The AG gentamicin was shown to activate the Cpx response [50]. As a corollary, activation of Cpx leads to increased AG resistance. This was shown to be due to protection against AGs at the membrane [34, 51], partly through regulation of protein degradation at the inner membrane [49] and partly to downregulation of electron transport chains and iron import [34]. Cpx was in fact described to repress *nuo* and *cyo* aerobic respiratory complexes in *E. coli* [47], which could be toxic in conditions challenging membrane integrity, and such repression allows bacterial cells to adapt to conditions disrupting membrane integrity, among which AG induced protein misfolding. There are no described sequence homologues for *nuo* or *cyo* operons in *V. cholerae*. The functional equivalent may be the *nqr* system [52](VC_2291-2-3-4), for which we see that inactivation is beneficial in WT TOB but not in *Δravvia* TOB, maybe because it is already down-regulated (approximately 2-fold but with *p-value* > 0,05) in *Δravvia*.

Since the Cpx response is involved in the biogenesis of large complexes present at the envelope (respiratory complexes, but also type 4 pili, and maybe others), one could envisage that the action of Cpx may be through reduced protein trafficking at the inner membrane, hence reduced membrane stress. These properties - decrease of respiration and iron import by Cpx - can explain how ROS formation increases in *Δravvia* upon *cpx* deletion, because ROS are mainly produced with oxygen and iron through the Fenton reaction. Cpx is also closely linked to energy status of the cell and regulates protein folding and degrading factors, which are involved in adaptation to stress caused by high level of respiration[53].

In *E. coli*, ZraPSR is involved in resistance to several drugs and is important for membrane integrity[25]. Zra chaperone activity is enhanced by zinc. There is often significant overlap between processes affected by Zinc and by ROS, with zinc having mostly antioxidant function [54]. *Δzra* has increased membrane disruption during treatment with membrane targeting antibiotics. ChIP-seq and

transcriptomic studies found that Zra controls the expression of *acr*, *raiA*, *rpoH*, etc. In *V. cholerae*, we find that the operon VC_1314-VC_1315-VC_1316 is highly upregulated in Δ *ravvia*. Although VC_1314 (487 aa) does not present any sequence homology to neither *zra* nor *cpx* systems, VC_1315 (449 aa) and VC_1316 (158 aa) present homologies respectively with *E. coli zraS* (465 aa) and *cpxR* (232 aa). Since the *V. cholerae* VC_1314-VC_1315-VC_1316 *zra*-like system also responds to zinc, we propose to name it *zraP2-zraS2-zraR2*.

One question remains open: why does deletion of the RavA-ViaA function activate the Cpx/Zra2 systems? The answer could come from the fact that when both RavA-ViaA and Cpx or Zra2 are inactivated, membrane permeability increases as observed with vancomycin and nitrocefin entry. The mechanism could be a complex one, since we also observe that RNA modifications, which impact translation [19], also impact Δ *ravvia* phenotypes. Note that *V. cholerae* harbors two *groESL* operons, with *gro1* being essential and *gro2* accessory. We have recently shown the involvement of *gro2* in the response to AGs [28]. Here, even in the absence of AGs, *gro2* is already essential for Δ *ravvia*. A specific target of this chaperone may be important in the absence of *ravvia*. Δ *ravvia* increases resistance to AGs but the importance of *gro2* and *clpS* may point to the existence of endogenous membrane protein stress in Δ *ravvia*. Thus, the presence of RavA-ViaA seems to be useful in order to maintain envelope integrity, and its function as a barrier against the entry of exogenous agents, such as the last resort antibiotic vancomycin.

Acknowledgements.

We thank Louna Fruchard for her help with flow cytometry experiments. We thank Frédéric Barras for critical reading of the manuscript, Jessica El Khoury and Eduardo Rocha and Béatrice Py for valuable discussions, and Dominique Fourmy for the gift of Neo-Cy5. We also thank, for RNA-seq experiments, E. Turc, L. Lemée, T. Cokelaer, Biomics Platform and C2RT (Institut Pasteur, Paris, France, supported by France Génomique (ANR-10-INBS-09) and IBISA. We thank Sebastian Aguilar Pierlé for help with TN-seq analysis.

This research was funded by the Institut Pasteur, the Centre National de la Recherche Scientifique (CNRS-UMR 3525), the Institut Pasteur grant PTR 245-19, ANR ModRNAntibio (ANR-21-CE35-0012), ANR-LabEx [ANR-10-LABX-62-IBEID], the Fondation pour la Recherche Médicale (FRM EQU202103012569). AB was funded by Institut Pasteur Roux-Cantarini fellowship.

Materials and methods

Table S5 shows strains used in this study and their construction.

Table S6 shows primer sequences.

Media and Growth Conditions

Platings were done at 37°C, in Mueller-Hinton (MH) agar media. Liquid cultures were grown at 37°C in MH in aerobic conditions, with 180 rotations per minute.

Statistical significance. For multiple comparisons, we used one-way ANOVA. **** means $p < 0.0001$, *** means $p < 0.001$, ** means $p < 0.01$, * means $p < 0.05$. ns: non-significant. All statistical tests were corrected for multiple comparisons and false discovery using the Bonferroni correction.

Competition experiments were performed as described[19]: overnight cultures from single colonies of mutant *lacZ*- and WT *lacZ*+ strains were mixed 1:1 (500 μ l + 500 μ l). At this point 100 μ l of the mix

were serially diluted and plated on MH agar supplemented with X-gal (5-bromo-4-chloro-3-indolyl- β -D-galactopyranoside) at 40 μ g/ml to assess T0 initial 1:1 ratio. At the same time, 5 μ l from the mix were added to 200 μ l of MH or MH supplemented with sub-MIC antibiotics (concentrations, unless indicated otherwise: TOB: tobramycin 0.6 μ g/ml; GEN: 0.5 μ g/ml; CIP: ciprofloxacin 0.01 μ g/ml, CRB: carbenicillin 2.5 μ g/ml), PQ: paraquat 10 μ M, or H₂O₂: 2 mM). Cultures were incubated in 96 well plates with agitation at 37°C for 24 hours, and then diluted and plated on MH agar plates supplemented with X-gal. Plates were incubated overnight at 37°C and the number of blue and white CFUs was assessed. Competitive index was calculated by dividing the number of white CFUs (Δ *lacZ*- strain) by the number of blue CFUs (*lacZ*+ strain) and normalizing this ratio to the T0 initial ratio.

MIC determination

Stationary phase cultures grown in MH were diluted 20 times in PBS, and 300 μ l were plated on MH plates and dried for 10 minutes. Etest strips (Biomérieux) were placed on the plates and incubated overnight at 37°C.

Survival/tolerance tests were performed on early exponential phase cultures. The overnight stationary phase cultures were diluted 1000X and grown until OD 600 nm of 0.35 to 0.4, at 37°C with shaking, in Erlenmeyers containing 25 ml fresh MH medium. Appropriate dilutions were plated on MH plates to determine the total number of CFUs in time zero untreated cultures. 5 ml of cultures were collected into 50 ml Falcon tubes and treated with lethal doses of desired antibiotics (5 or 10 times the MIC: tobramycin 5 or 10 μ g/ml, carbenicillin 50 μ g/ml, ciprofloxacin 0.025 μ g/ml) for 30 min, 1 hour, 2 hours and 4 hours if needed, at 37°C with shaking in order to guarantee oxygenation. Appropriate dilutions were then plated on MH agar without antibiotics and proportion of growing CFUs were calculated by doing a ratio with total CFUs at time zero. Experiments were performed 3 to 8 times.

Quantification of fluorescent neomycin uptake was performed as described [29]. Neo-Cy5 is an aminoglycoside coupled to the fluorophore Cy5, and has been shown to be active against Gram-bacteria [31, 55]. Briefly, overnight cultures were diluted 100-fold in rich MOPS (Teknova EZ rich defined medium). When the bacterial strains reached an OD 600 nm of ~0.25, they were incubated with 0.4 μ M of Cy5 labeled neomycin for 15 minutes at 37°C. 10 μ l of the incubated culture were then used for flow cytometry, diluting them in 250 μ l of PBS before reading fluorescence. WT *V. cholerae*, was incubated simultaneously without Neo-Cy5 as a negative control. Flow cytometry experiments were performed as described [56] and repeated at least 3 times. For each experiment, 100000 events were counted on the Miltenyi MACSquant device.

PMF measurements

Quantification of PMF was performed using the Mitotracker Red CMXRos dye (Invitrogen) as described [32], in parallel with the neo-Cy5 uptake assay, using the same bacterial cultures. 50 μ l of each culture were mixed with 60 μ l of PBS. Tetrachlorosalicylanilide TCS (ThermoFischer), a protonophore, was used as a negative control with a 500 μ M treatment applied for 10 minutes at room temperature. Then, 25 nM of Mitotracker Red were added to each sample and let at room temperature for 15 minutes under aluminium foil. 20 μ L of the treated culture were then used for flow cytometry, diluted in 200 μ L of PBS before reading fluorescence.

ROS measurements

Overnight cultures were diluted 1000X in MH medium and grown until an OD 600 nm of 0.3. Then, 100 μ l of each culture was transferred to a 96-well plate, and treated with 1 μ l of 250 μ M CellRox Green (ThermoFischer Scientific), for 30 minutes at 37 degrees, under aluminium foil. For flow cytometry,

10 μ l were mixed into 200 μ l of PBS. Fluorescence per cell was read on 100000 events, on the MACSquant device at 488 nm.

RNA purification and RNA-seq:

Cultures were diluted 1000X and grown in triplicate in MH to an OD 600 nm of 0.4. First, 1.5 ml of TriZol reagent was added to 500 μ l of culture pellet followed by the addition of 300 μ l of chloroforme. After centrifugation, the upper phase was mixed with a 1:1 volume of 70 % ethanol before column purification. RNA was purified with the RNeasy mini kit (Qiagen) according to manufacturer instruction (from step 4 of the protocole Part 1). Quality of RNA was controlled using the Bioanalyzer. Sample collection, total RNA extraction, library preparation, sequencing and analysis were performed as previously described [57].

Transposon insertion sequencing

Libraries were prepared as previously described [16, 58], to achieve a library size of 600000 clones, and subjected to passaging in MH and MH + TOB 0.5 μ g/ml for 16 generations [20]. A saturated mariner mutant library was generated by conjugation of plasmid pSC1819 from *E. coli* to *V. cholerae* WT. Briefly, pSC189 [16, 58] was delivered from *E. coli* strain 7257 (β 2163 pSC189::spec, laboratory collection) into the *V. cholerae* WT strain. Conjugation was performed for 2 h on 0.45 μ M filters. The filter was resuspended in 2 ml of MH broth. Petri dishes containing 100 μ g/ml spectinomycin were then spread. The colonies were scraped and resuspended in 2 ml of MH. When sufficient single mutants were obtained (>600000 for 6X coverage of non-essential regions), a portion of the library was used for gDNA extraction using Qiagen DNeasy Blood & Tissue Kit as per manufacturer's instructions. This was used for library validation through insert amplification by nested PCR using a degenerate primer (ARB6), which contains 20 defined nucleotides followed by a randomized sequence. This was combined with a primer anchored in the edge of the transposon sequence (MV288) [16, 20]. After this, primer ARB3, which contains the first 20 nucleotides of ARB6 was used for nested amplification in combination with MV288. After validation, the libraries were passaged in MH media for 16 generations with or without 50 % MIC of TOB, in triplicates. gDNA from time point 0 and both conditions after 16 generation passage in triplicate was extracted. Sequencing libraries were prepared using Agilent's SureSelect XT2 Kit with custom RNA baits designed to hybridize the edges of the Mariner transposon. The 100 ng protocol was followed as per manufacturer's instructions. A total of 12 cycles were used for library amplification. Agilent's 2100 Bioanalyzer was used to verify the size of the pooled libraries and their concentration. HiSeq Paired-end Illumina sequencing technology was used producing 2 x 125 bp long reads. Reads were then filtered through transposon mapping to ensure the presence of an informative transposon/genome junction using a previously described mapping algorithm [59]. Informative reads were extracted and mapped. Reads were counted when the junction was reported as mapped inside the CDS of a gene plus an additional 50 bp upstream and downstream. Expansion or decrease of fitness of mutants was calculated in fold changes with normalized insertion numbers. Normalization calculations were applied according to van Opijnen et al [60]. Expansion or decrease of fitness of mutants was calculated in fold changes with normalized insertion numbers. Baggerly's test on proportions [61] was used to determine statistical significance as well as a Bonferroni correction for multiple hypotheses testing.

mRNA quantifications by digital-RT-PCR

qRT-PCR reactions were prepared with 1 μ l of diluted RNA samples using the qScript XLT 1-Step RT-qPCR ToughMix (Quanta Biosciences, Gaithersburg, MD, USA) within Sapphire chips. Digital PCR was conducted on a Naica Geode (programmed to perform the sample partitioning step into droplets, followed by the thermal cycling program suggested in the user's manual. Image acquisition was

performed using the Naica Prism3 reader. Images were then analyzed using Crystal Reader software (total droplet enumeration and droplet quality control) and the Crystal Miner software (extracted fluorescence values for each droplet). Values were normalized against expression of the housekeeping gene *gyrA* as previously described [62].

Quantification of *gfp* fusion expression by fluorescent flow cytometry

Flow cytometry experiments were performed as described [56] on overnight cultures and repeated at least 3 times. For each experiment, 50000 to 100000 events were counted on the Miltenyi MACSquant device.

Transcriptional fusion: *ravvia* promoter sequence fused to *gfp* by amplification of *Pravvia-gfp* from pZE1-*gfp* [63] using primers ZIP537/ZIP200. The fragment was cloned into pTOPO-TA cloning vector. The *Pravvia-gfp* fragment was then extracted using *EcoRI* and cloned into the low copy plasmid pSC101. The plasmid was introduced into desired strains, and fluorescence was measured on indicated conditions, by counting 100000 cells on the Miltenyi MACSquant device

Growth on microtiter plate reader

Overnight cultures were diluted 1:500 in fresh MH medium, on 96 well plates. Each well contained 200 μ l. Plates were incubated with shaking on TECAN plate reader device at 37°C, OD 600 nm was measured every 15 minutes. Tobramycin was used at sub-MIC: TOB 0.6 μ g/ml. The concentrations of other antibiotics are specified on each figure.

Quantification of nitrocefin entry.

Nitrocefin, a chromogenic probe, 3-(2,4-dinitrostyryl)-(6 R,7 R)-7-(2-thienylacetamido)-ceph-3-em-4-carboxyl acid (Calbiochem), was used to assess membrane permeability. Tested strains were transformed with the low copy pSC101 plasmid carrying the *bla* gene coding for a β -lactamase, a periplasmic protein which allows coloration of nitrocefin upon entry into the bacterial cell. Cells were grown to stationary phase, washed twice and resuspended at a concentration of 5×10^7 cells/ml in PBS. The reaction was performed with 175 μ l of PBS buffer and 25 μ l of the nitrocefin 0.5 mg/ml stock solution, in 96 well plates. 50 μ l of the bacterial suspension was added and the OD at 490 nm was measured every 2 min for 45 min using a plate reader at 37°C, with shaking for 10 s every minute.

Data availability: The data discussed in this publication have been deposited in NCBI's Gene Expression Omnibus and are accessible through GEO Series accession number GSE196651 (GSM5897403, GSM5897404, GSM5897405, GSM5897412, GSM5897413, GSM5897414) for RNAseq data and GSE198341 for TNseq data (GSM5945317, GSM5945318, GSM5945319, GSM5945323, GSM5945324, GSM5945325, GSM5945329, GSM5945330, GSM5945331, GSM5945338, GSM5945339, GSM5945340, GSM5945341, GSM5945342, GSM5945343).

Table 1

MIC $\mu\text{g/ml}$	MH
<i>Δravvia</i>	1.2-1.5
WT:: <i>ravviaOE+</i>	0.75
<i>ΔravA</i>	1.2-1.5
<i>ΔviaA</i>	1.2-1.5
WT	1.2

Table S1. RNA-seq

Table S2. Transposon insertion sequencing at time T0: genes that cannot be inactivated only in WT or only in *Δ ravvia*

Table S3. Transposon insertion sequencing at time T16, with no treatment: genes that tolerate more insertions either in WT or in *Δ ravvia*

Table S4. Transposon insertion sequencing at time T16, with sub-MIC TOB: genes that tolerate more insertions either in WT or in *Δ ravvia*

Table S5: Strains

Table S6: Plasmids

References

1. Lortholary O, Tod M, Cohen Y, Petitjean O. Aminoglycosides. *Med Clin North Am.* 1995;79(4):761-87. PubMed PMID: 7791422.
2. Davis BD. Mechanism of bactericidal action of aminoglycosides. *Microbiol Rev.* 1987;51(3):341-50. PubMed PMID: 3312985; PubMed Central PMCID: PMC373115.
3. Davis. Mechanism of bactericidal action of aminoglycosides. *Microbiol Rev.* 1988;52(1):153. PubMed PMID: 16350244; PubMed Central PMCID: PMC372710.
4. Fraimow HS, Greenman JB, Leviton IM, Dougherty TJ, Miller MH. Tobramycin uptake in *Escherichia coli* is driven by either electrical potential or ATP. *J Bacteriol.* 1991;173(9):2800-8. PubMed PMID: 2019557; PubMed Central PMCID: PMC207860.
5. Herisse M, Duverger Y, Martin-Verstraete I, Barras F, Ezraty B. Silver potentiates aminoglycoside toxicity by enhancing their uptake. *Mol Microbiol.* 2017;105(1):115-26. doi: 10.1111/mmi.13687. PubMed PMID: 28383153.
6. Taber HW, Mueller JP, Miller PF, Arrow AS. Bacterial uptake of aminoglycoside antibiotics. *Microbiol Rev.* 1987;51(4):439-57. PubMed PMID: 3325794; PubMed Central PMCID: PMC373126.
7. Bryan LE, Van Den Elzen HM. Effects of membrane-energy mutations and cations on streptomycin and gentamicin accumulation by bacteria: a model for entry of streptomycin and gentamicin in susceptible and resistant bacteria. *Antimicrob Agents Chemother.* 1977;12(2):163-77. PubMed PMID: 143238; PubMed Central PMCID: PMC429880.
8. Nichols WW, Young SN. Respiration-dependent uptake of dihydrostreptomycin by *Escherichia coli*. Its irreversible nature and lack of evidence for a uniport process. *Biochem J.* 1985;228(2):505-12. PubMed PMID: 2409962; PubMed Central PMCID: PMC1145009.
9. Alper MD, Ames BN. Transport of antibiotics and metabolite analogs by systems under cyclic AMP control: positive selection of *Salmonella typhimurium* *cya* and *crp* mutants. *J Bacteriol.* 1978;133(1):149-57. PubMed PMID: 201606; PubMed Central PMCID: PMC221988.
10. Davis BD, Chen LL, Tai PC. Misread protein creates membrane channels: an essential step in the bactericidal action of aminoglycosides. *Proc Natl Acad Sci U S A.* 1986;83(16):6164-8. PubMed PMID: 2426712; PubMed Central PMCID: PMC386460.
11. Wong KS, Snider JD, Graham C, Greenblatt JF, Emili A, Babu M, et al. The MoxR ATPase RavA and its cofactor ViaA interact with the NADH:ubiquinone oxidoreductase I in *Escherichia coli*. *PLoS One.* 2014;9(1):e85529. doi: 10.1371/journal.pone.0085529. PubMed PMID: 24454883; PubMed Central PMCID: PMC3893208.
12. Kandiah E, Carriel D, Perard J, Malet H, Bacia M, Liu K, et al. Structural insights into the *Escherichia coli* lysine decarboxylases and molecular determinants of interaction with the AAA+ ATPase RavA. *Scientific reports.* 2016;6:24601. doi: 10.1038/srep24601. PubMed PMID: 27080013; PubMed Central PMCID: PMC4832331.
13. Snider J, Gutsche I, Lin M, Baby S, Cox B, Butland G, et al. Formation of a distinctive complex between the inducible bacterial lysine decarboxylase and a novel AAA+ ATPase. *J Biol Chem.* 2006;281(3):1532-46. doi: 10.1074/jbc.M511172200. PubMed PMID: 16301313.
14. Jessop M, Arragain B, Miras R, Fraudeau A, Huard K, Bacia-Verloop M, et al. Structural insights into ATP hydrolysis by the MoxR ATPase RavA and the LdcI-RavA cage-like complex. *Commun Biol.* 2020;3(1):46. Epub 2020/01/30. doi: 10.1038/s42003-020-0772-0. PubMed PMID: 31992852; PubMed Central PMCID: PMC6987120.
15. Felix J, Bumba L, Liesche C, Fraudeau A, Rebeille F, El Khoury JY, et al. The AAA+ ATPase RavA and its binding partner ViaA modulate *E. coli* aminoglycoside sensitivity through interaction with the inner membrane. *Nature communications.* 2022;13(1):5502. Epub 2022/09/21. doi: 10.1038/s41467-022-32992-9. PubMed PMID: 36127320; PubMed Central PMCID: PMC9489729.
16. Baharoglu Z, Babosan A, Mazel D. Identification of genes involved in low aminoglycoside-induced SOS response in *Vibrio cholerae*: a role for transcription stalling and Mfd helicase. *Nucleic*

- Acids Res. 2014;42(4):2366-79. Epub 2013/12/10. doi: 10.1093/nar/gkt1259. PubMed PMID: 24319148; PubMed Central PMCID: PMCPMC3936754.
17. Girgis HS, Hottes AK, Tavazoie S. Genetic architecture of intrinsic antibiotic susceptibility. PLoS One. 2009;4(5):e5629. doi: 10.1371/journal.pone.0005629. PubMed PMID: 19462005; PubMed Central PMCID: PMCPMC2680486.
18. Khoury JYE, Beas JZ, Huguenot A, Py B, Barras F. Bioenergetic State of Escherichia coli Controls Aminoglycoside Susceptibility. mBio. 0(0):e03302-22. doi: doi:10.1128/mbio.03302-22.
19. Babosan A, Fruchard L, Krin E, Carvalho A, Mazel D, Baharoglu Z. Non-essential tRNA and rRNA modifications impact the bacterial response to sub-MIC antibiotic stress. microLife. 2022. doi: 10.1093/femsml/uqac019.
20. Negro V, Krin E, Aguilar Pierle S, Chaze T, Gai Gianetto Q, Kennedy SP, et al. RadD Contributes to R-Loop Avoidance in Sub-MIC Tobramycin. MBio. 2019;10(4). doi: 10.1128/mBio.01173-19. PubMed PMID: 31266870; PubMed Central PMCID: PMCPMC6606805.
21. Eisenberg ES, Mandel LJ, Kaback HR, Miller MH. Quantitative association between electrical potential across the cytoplasmic membrane and early gentamicin uptake and killing in Staphylococcus aureus. J Bacteriol. 1984;157(3):863-7. PubMed PMID: 6698939; PubMed Central PMCID: PMCPMC215339.
22. Ezraty B, Vergnes A, Banzhaf M, Duverger Y, Huguenot A, Brochado AR, et al. Fe-S cluster biosynthesis controls uptake of aminoglycosides in a ROS-less death pathway. Science. 2013;340(6140):1583-7. Epub 2013/07/03. doi: 340/6140/1583 [pii] 10.1126/science.1238328. PubMed PMID: 23812717.
23. Babu M, Arnold R, Bundalovic-Torma C, Gagarinova A, Wong KS, Kumar A, et al. Quantitative genome-wide genetic interaction screens reveal global epistatic relationships of protein complexes in Escherichia coli. PLoS Genet. 2014;10(2):e1004120. doi: 10.1371/journal.pgen.1004120. PubMed PMID: 24586182; PubMed Central PMCID: PMCPMC3930520.
24. Grabowicz M, Silhavy TJ. Envelope Stress Responses: An Interconnected Safety Net. Trends Biochem Sci. 2017;42(3):232-42. Epub 2016/11/15. doi: 10.1016/j.tibs.2016.10.002. PubMed PMID: 27839654; PubMed Central PMCID: PMCPMC5336467.
25. Rome K, Borde C, Taher R, Cayron J, Lesterlin C, Gueguen E, et al. The Two-Component System ZraPSR Is a Novel ESR that Contributes to Intrinsic Antibiotic Tolerance in Escherichia coli. J Mol Biol. 2018;430(24):4971-85. Epub 2018/11/06. doi: 10.1016/j.jmb.2018.10.021. PubMed PMID: 30389436.
26. Petit-Hartlein I, Rome K, de Rosny E, Molton F, Duboc C, Gueguen E, et al. Biophysical and physiological characterization of ZraP from Escherichia coli, the periplasmic accessory protein of the atypical ZraSR two-component system. Biochem J. 2015;472(2):205-16. Epub 2015/10/07. doi: 10.1042/BJ20150827. PubMed PMID: 26438879.
27. Balaban NQ, Helaine S, Lewis K, Ackermann M, Aldridge B, Andersson DI, et al. Definitions and guidelines for research on antibiotic persistence. Nat Rev Microbiol. 2019;17(7):441-8. Epub 2019/04/14. doi: 10.1038/s41579-019-0196-3. PubMed PMID: 30980069; PubMed Central PMCID: PMCPMC7136161.
28. Carvalho A, Mazel D, Baharoglu Z. Deficiency in cytosine DNA methylation leads to high chaperonin expression and tolerance to aminoglycosides in Vibrio cholerae. Plos Genetics. 2021;17(10). doi: ARTN e1009748 10.1371/journal.pgen.1009748. PubMed PMID: WOS:000710679300002.
29. Lang MN, Krin E, Korlowski C, Sismeiro O, Varet H, Coppee JY, et al. Sleeping ribosomes: Bacterial signaling triggers RaiA mediated persistence to aminoglycosides. Iscience. 2021;24(10). doi: ARTN 103128 10.1016/j.isci.2021.103128. PubMed PMID: WOS:000713815900006.
30. Pierlé SA, Lang M, López-Igual R, Krin E, Fourmy D, Kennedy SP, et al. Identification of the active mechanism of aminoglycoside entry in *V. cholerae* through characterization of

- sRNA *ctrR* regulating carbohydrate utilization and transport. bioRxiv. 2023:2023.07.19.549712. doi: 10.1101/2023.07.19.549712.
31. Sabeti Azad M, Okuda M, Cyrenne M, Bourge M, Heck MP, Yoshizawa S, et al. Fluorescent aminoglycoside antibiotics and methods for accurately monitoring uptake by bacteria. *ACS Infect Dis*. 2020. Epub 2020/03/21. doi: 10.1021/acsinfecdis.9b00421. PubMed PMID: 32195576.
 32. El Mortaji L, Tejada-Arranz A, Rifflet A, Boneca IG, Pehau-Arnaudet G, Radicella JP, et al. A peptide of a type I toxin-antitoxin system induces *Helicobacter pylori* morphological transformation from spiral shape to coccoids. *Proc Natl Acad Sci U S A*. 2020;117(49):31398-409. Epub 2020/11/25. doi: 10.1073/pnas.2016195117. PubMed PMID: 33229580; PubMed Central PMCID: PMC7733810.
 33. Wong KS, Bhandari V, Janga SC, Houry WA. The RavA-ViaA Chaperone-Like System Interacts with and Modulates the Activity of the Fumarate Reductase Respiratory Complex. *J Mol Biol*. 2017;429(2):324-44. Epub 2016/12/17. doi: 10.1016/j.jmb.2016.12.008. PubMed PMID: 27979649.
 34. Raivio TL, Leblanc SK, Price NL. The *Escherichia coli* Cpx envelope stress response regulates genes of diverse function that impact antibiotic resistance and membrane integrity. *J Bacteriol*. 2013;195(12):2755-67. Epub 2013/04/09. doi: 10.1128/JB.00105-13. PubMed PMID: 23564175; PubMed Central PMCID: PMC3697260.
 35. Baharoglu Z, Krin E, Mazel D. RpoS Plays a Central Role in the SOS Induction by Sub-Lethal Aminoglycoside Concentrations in *Vibrio cholerae*. *Plos Genetics*. 2013;9(4). doi: 10.1371/journal.pgen.1003421. PubMed PMID: WOS:000318073300017.
 36. Delcour AH. Outer membrane permeability and antibiotic resistance. *Biochim Biophys Acta*. 2009;1794(5):808-16. Epub 2008/12/23. doi: 10.1016/j.bbapap.2008.11.005. PubMed PMID: 19100346; PubMed Central PMCID: PMC2696358.
 37. Song M, Liu Y, Huang X, Ding S, Wang Y, Shen J, et al. A broad-spectrum antibiotic adjuvant reverses multidrug-resistant Gram-negative pathogens. *Nat Microbiol*. 2020;5(8):1040-50. Epub 2020/05/20. doi: 10.1038/s41564-020-0723-z. PubMed PMID: 32424338.
 38. Lei E, Tao H, Jiao S, Yang A, Zhou Y, Wang M, et al. Potentiation of Vancomycin: Creating Cooperative Membrane Lysis through a "Derivatization-for-Sensitization" Approach. *J Am Chem Soc*. 2022;144(23):10622-39. Epub 2022/06/04. doi: 10.1021/jacs.2c03784. PubMed PMID: 35657057.
 39. Mathur J, Waldor MK. The *Vibrio cholerae* ToxR-regulated porin OmpU confers resistance to antimicrobial peptides. *Infect Immun*. 2004;72(6):3577-83. Epub 2004/05/25. doi: 10.1128/IAI.72.6.3577-3583.2004. PubMed PMID: 15155667; PubMed Central PMCID: PMC415678.
 40. Acosta N, Pukatzki S, Raivio TL. The *Vibrio cholerae* Cpx envelope stress response senses and mediates adaptation to low iron. *J Bacteriol*. 2015;197(2):262-76. Epub 2014/11/05. doi: 10.1128/JB.01957-14. PubMed PMID: 25368298; PubMed Central PMCID: PMC4272599.
 41. Buelow DR, Raivio TL. Cpx signal transduction is influenced by a conserved N-terminal domain in the novel inhibitor CpxP and the periplasmic protease DegP. *J Bacteriol*. 2005;187(19):6622-30. Epub 2005/09/17. doi: 10.1128/JB.187.19.6622-6630.2005. PubMed PMID: 16166523; PubMed Central PMCID: PMC1251582.
 42. Raivio TL, Laird MW, Joly JC, Silhavy TJ. Tethering of CpxP to the inner membrane prevents spheroplast induction of the cpx envelope stress response. *Mol Microbiol*. 2000;37(5):1186-97. Epub 2000/09/06. doi: 10.1046/j.1365-2958.2000.02074.x. PubMed PMID: 10972835.
 43. Raivio TL, Popkin DL, Silhavy TJ. The Cpx envelope stress response is controlled by amplification and feedback inhibition. *J Bacteriol*. 1999;181(17):5263-72. Epub 1999/08/28. doi: 10.1128/JB.181.17.5263-5272.1999. PubMed PMID: 10464196; PubMed Central PMCID: PMC94031.
 44. DiGiuseppe PA, Silhavy TJ. Signal detection and target gene induction by the CpxRA two-component system. *J Bacteriol*. 2003;185(8):2432-40. Epub 2003/04/03. doi: 10.1128/JB.185.8.2432-2440.2003. PubMed PMID: 12670966; PubMed Central PMCID: PMC152615.

45. Thorbjarnardottir SH, Magnusdottir RA, Eggertsson G. Mutations determining generalized resistance to aminoglycoside antibiotics in *Escherichia coli*. *Mol Gen Genet*. 1978;161(1):89-98. Epub 1978/04/25. doi: 10.1007/BF00266619. PubMed PMID: 353502.
46. Cudic E, Surmann K, Panasia G, Hammer E, Hunke S. The role of the two-component systems Cpx and Arc in protein alterations upon gentamicin treatment in *Escherichia coli*. *BMC Microbiol*. 2017;17(1):197. Epub 2017/09/20. doi: 10.1186/s12866-017-1100-9. PubMed PMID: 28923010; PubMed Central PMCID: PMC5604497.
47. Guest RL, Wang J, Wong JL, Raivio TL. A Bacterial Stress Response Regulates Respiratory Protein Complexes To Control Envelope Stress Adaptation. *J Bacteriol*. 2017;199(20). Epub 2017/08/02. doi: 10.1128/JB.00153-17. PubMed PMID: 28760851; PubMed Central PMCID: PMC5637174.
48. Jing W, Liu J, Wu S, Li X, Liu Y. Role of cpxA Mutations in the Resistance to Aminoglycosides and beta-Lactams in *Salmonella enterica* serovar Typhimurium. *Front Microbiol*. 2021;12:604079. Epub 2021/02/23. doi: 10.3389/fmicb.2021.604079. PubMed PMID: 33613478; PubMed Central PMCID: PMC7889517.
49. Raivio TL. Everything old is new again: an update on current research on the Cpx envelope stress response. *Biochim Biophys Acta*. 2014;1843(8):1529-41. Epub 2013/11/05. doi: 10.1016/j.bbamcr.2013.10.018. PubMed PMID: 24184210.
50. Kashyap DR, Kuzma M, Kowalczyk DA, Gupta D, Dziarski R. Bactericidal peptidoglycan recognition protein induces oxidative stress in *Escherichia coli* through a block in respiratory chain and increase in central carbon catabolism. *Mol Microbiol*. 2017;105(5):755-76. Epub 2017/06/18. doi: 10.1111/mmi.13733. PubMed PMID: 28621879; PubMed Central PMCID: PMC5570643.
51. Mahoney TF, Silhavy TJ. The Cpx stress response confers resistance to some, but not all, bactericidal antibiotics. *J Bacteriol*. 2013;195(9):1869-74. Epub 2013/01/22. doi: 10.1128/JB.02197-12. PubMed PMID: 23335416; PubMed Central PMCID: PMC3624577.
52. Agarwal S, Bernt M, Toulouse C, Kurz H, Pfannstiel J, D'Alvise P, et al. Impact of Na(+)-Translocating NADH:Quinone Oxidoreductase on Iron Uptake and nqrM Expression in *Vibrio cholerae*. *J Bacteriol*. 2020;202(3). Epub 2019/11/13. doi: 10.1128/JB.00681-19. PubMed PMID: 31712283; PubMed Central PMCID: PMC6964743.
53. Tsviklist V, Guest RL, Raivio TL. The Cpx Stress Response Regulates Turnover of Respiratory Chain Proteins at the Inner Membrane of *Escherichia coli*. *Front Microbiol*. 2021;12:732288. Epub 2022/02/15. doi: 10.3389/fmicb.2021.732288. PubMed PMID: 35154019; PubMed Central PMCID: PMC8831704.
54. Hubner C, Haase H. Interactions of zinc- and redox-signaling pathways. *Redox Biol*. 2021;41:101916. Epub 2021/03/05. doi: 10.1016/j.redox.2021.101916. PubMed PMID: 33662875; PubMed Central PMCID: PMC7937829.
55. Okuda M. Mechanism of action of a class of antibiotics from their entry to their target in bacteria : a real time visualization: Université Paris Sud - Paris XI; 2015.
56. Baharoglu Z, Bikard D, Mazel D. Conjugative DNA transfer induces the bacterial SOS response and promotes antibiotic resistance development through integron activation. *PLoS Genet*. 2010;6(10):e1001165. Epub 2010/10/27. doi: 10.1371/journal.pgen.1001165. PubMed PMID: 20975940; PubMed Central PMCID: PMC2958807.
57. Krin E, Pierle SA, Sismeiro O, Jagla B, Dillies MA, Varet H, et al. Expansion of the SOS regulon of *Vibrio cholerae* through extensive transcriptome analysis and experimental validation. *BMC Genomics*. 2018;19(1):373. doi: 10.1186/s12864-018-4716-8. PubMed PMID: 29783948; PubMed Central PMCID: PMC5963079.
58. Chiang SL, Rubin EJ. Construction of a mariner-based transposon for epitope-tagging and genomic targeting. *Gene*. 2002;296(1-2):179-85. Epub 2002/10/18. doi: S0378111902008569 [pii]. PubMed PMID: 12383515.
59. Pierle SA, Rosshandler II, Kerudin AA, Sambono J, Lew-Tabor A, Rolls P, et al. Genetic Diversity of Tick-Borne Rickettsial Pathogens; Insights Gained from Distant Strains. *Pathogens*.

2014;3(1):57-72. doi: 10.3390/pathogens3010057. PubMed PMID: 25364572; PubMed Central PMCID: PMC4213813.

60. van Opijnen T, Bodi KL, Camilli A. Tn-seq: high-throughput parallel sequencing for fitness and genetic interaction studies in microorganisms. *Nat Methods*. 2009;6(10):767-72. doi: 10.1038/nmeth.1377. PubMed PMID: 19767758; PubMed Central PMCID: PMC2957483.

61. Baggerly KA, Deng L, Morris JS, Aldaz CM. Differential expression in SAGE: accounting for normal between-library variation. *Bioinformatics*. 2003;19(12):1477-83. PubMed PMID: 12912827.

62. Lo Scrudato M, Blokesch M. The regulatory network of natural competence and transformation of *Vibrio cholerae*. *PLoS Genet*. 2012;8(6):e1002778. Epub 2012/06/28. doi: 10.1371/journal.pgen.1002778

PGENETICS-D-12-00108 [pii]. PubMed PMID: 22737089; PubMed Central PMCID: PMC3380833.

63. Elowitz MB, Leibler S. A synthetic oscillatory network of transcriptional regulators. *Nature*. 2000;403(6767):335-8. Epub 2000/02/05. doi: 10.1038/35002125. PubMed PMID: 10659856.

Main figure references

Figure 1: Effect of RavA-ViaA on fitness and tolerance to aminoglycosides. A. Competition experiments mixing *ravvia* deletion (Δ) and extra-copy (OE+) mutants and WT in indicated conditions. NT: non-treated. TOB: tobramycin. GEN: gentamicin. CM: chloramphenicol. CIP: ciprofloxacin. The Y-axis represents \log_2 of competitive index value calculated as described in the methods. A competitive index of 1 (i.e. \log_2 value of 0) indicates equal growth of both strains. For statistical significance calculations, we used one-way ANOVA. **** means $p < 0.0001$, *** means $p < 0.001$, ** means $p < 0.01$, * means $p < 0.05$. Only significant p values are shown. Number of replicates for each experiment: $3 < n < 8$. Concentrations are indicated in $\mu\text{g/ml}$. **B.** Survival of indicated strain to lethal tobramycin treatment. *V. cholerae* WT and deletion mutant cultures were grown without antibiotics up to early exponential phase, and serial dilutions were plated on MH medium without antibiotics. Exponential phase cultures were then treated with antibiotics at lethal concentrations for the indicated times. At each time point, dilutions were spotted on MH. Y-axis shows survival calculated as number of colonies at time TN divided by the initial number of colonies before antibiotic treatment. TOB: tobramycin 5 or 10 $\mu\text{g/ml}$.

Figure 2: Effect of RavA-ViaA on AG uptake and membrane potential. A. Intracellular level of neomycin coupled to the fluorophore Cy5 measured by fluorescence associated flow cytometry. Error bars represent standard deviation. **B.** Quantification of changes in PMF using Mitotracker Red fluorescence measured by flow cytometry. Representative acquisitions are shown: fluorescence is represented in the x-axis (FITC channel), the y-axis represents the number of events corresponding to the number of cells, normalized to height (same number of total cells for both conditions). Each plot represents one experiment. **C.** Competition experiments of *V. cholerae* WT and indicated mutants. MH: no antibiotic treatment (black). TOB: tobramycin 0,6 $\mu\text{g/ml}$ (blue). The Y-axis represents \log_2 of competitive index value calculated as described in the methods. A competitive index of 1 (i.e. \log_2 value of 0) indicates equal growth of both strains. For statistical significance calculations, we used one-way ANOVA. **** means $p < 0.0001$, *** means $p < 0.001$, ** means $p < 0.01$, * means $p < 0.05$. ns: non-significant. Number of replicates for each experiment: $n = 3$. Only significant p values are shown.

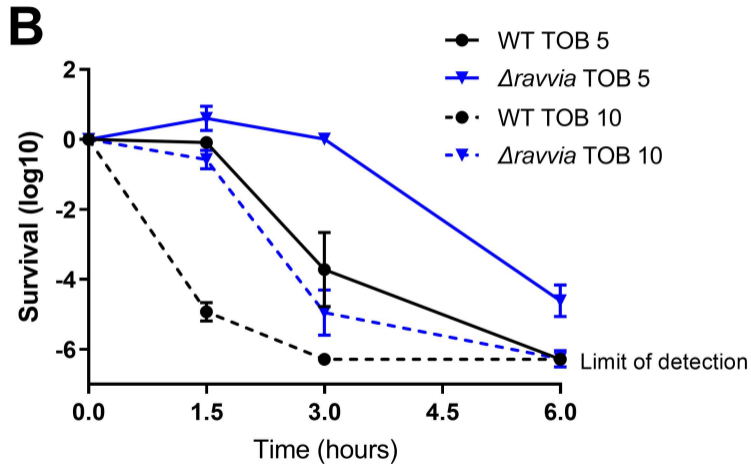
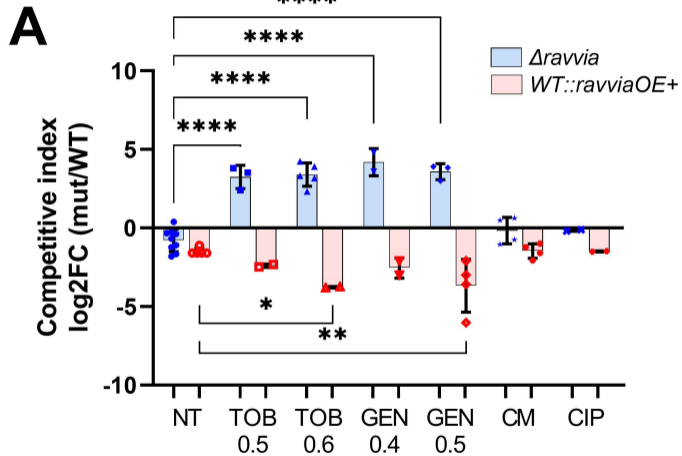
Figure 3: High throughput methods identify factors that are differentially detected in $\Delta ravvia$ compared to WT. Pie-chart for RNA-seq recapitulates differentially (up- or down-) expressed gene categories in $\Delta ravvia$, as shown in Table S1. Pie-chart for TN-seq recapitulates gene categories for differentially detected transposon insertions in $\Delta ravvia$ compared to WT, in all conditions shown in Tables S2, S3 and S4.

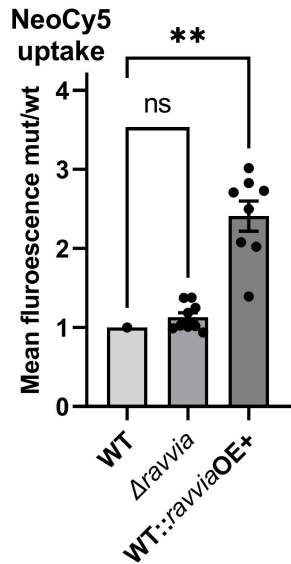
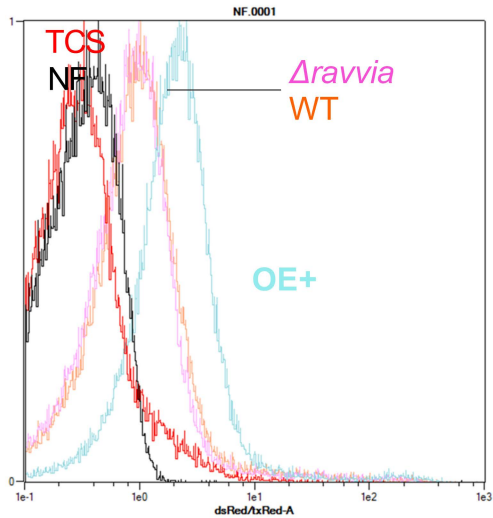
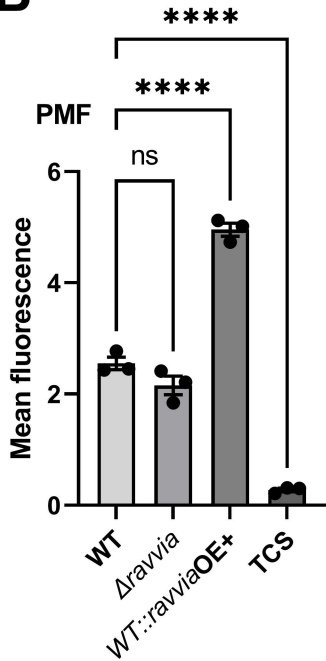
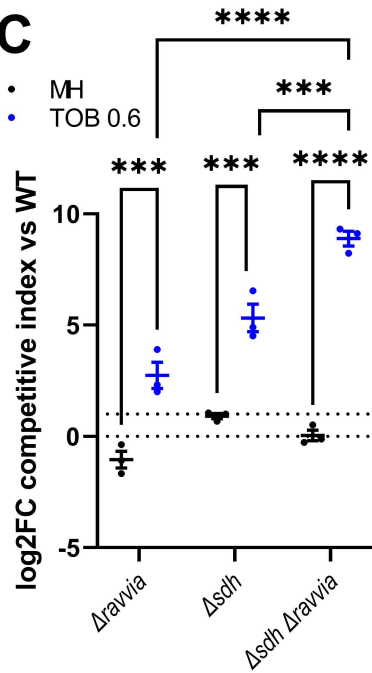
Figure 4: Cpx and Zra-like two component envelope stress response systems are involved in fitness increase of $\Delta ravvia$ with TOB and TOB tolerance. ABC. Competitions. The effect of deletion of *cpx* (A), or *zra-like* (B), or both (C) on competitive index in MH without and with TOB, where MH is the untreated growth medium. *In vitro* competition experiments of *V. cholerae* WT and indicated mutants in specified media: in black: MH: no antibiotic treatment. In blue: TOB: tobramycin 0,6 $\mu\text{g/ml}$. The Y-axis represents \log_2 of competitive index value calculated as described in the methods. A competitive index of 1 (i.e. \log_2 value of 0) indicates equal growth of both strains. **D.** Competitive index in MH without and with TOB, of the triple mutant (indicated as $\Delta\Delta\Delta$) $\Delta ravvia \Delta cpx \Delta zra$ against $\Delta ravvia \Delta cpx$. **E. Tolerance.** Cultures were grown to exponential phase in MH medium. Survival of WT and $\Delta ravvia$ to 3-hours treatment with lethal TOB at 5x MIC 5 $\mu\text{g/ml}$ was measured. The Y-axis represents \log_2 value of survival ratios, calculated as survival of the mutant over survival of the WT. A relative survival ratio of 1 (i.e. $\log_2 = 0$) indicates equal survival as the WT strain. For statistical significance calculations, we used one-way ANOVA. **** means $p < 0.0001$, *** means $p < 0.001$, ** means $p < 0.01$, * means $p < 0.05$. ns: non-significant. Number of replicates for each experiment: $3 < n < 8$.

Figure 5: Effect of zinc supplementation. ABC. Competitions. Cultures were grown to exponential phase in MH medium supplemented with zinc during growth. “Zn” stands for ZnCl₂: 1.5mM. The effect of deletion of *cpx* (A), or *zra-like* (B), or both (C) on competitive index in MH without and with TOB, where MH is the untreated growth medium. *In vitro* competition experiments of *V. cholerae* WT and indicated mutants in specified media: in black: MH: no antibiotic treatment. In blue: TOB: tobramycin 0,6 µg/ml. The Y-axis represents log₂ of competitive index value calculated as described in the methods. A competitive index of 1 (i.e. log₂ value of 0) indicates equal growth of both strains. **D. Survival** of WT and Δ *ravvia* to 3-hours treatment with lethal TOB at 5x MIC 5 µg/ml, in presence of zinc. The Y-axis represents log₂ value of survival rates ratios, calculated as survival of the mutant over survival of the WT. A relative survival ratio of 1 (i.e. log₂ = 0) indicates equal survival as the WT strain. **E. Expression of *cpx* and *zra*.** mRNA levels were measured using digital RT-PCR as explained in materials and methods. The Y-axis represents the fold change of induction in presence of zinc divided by the expression in the absence of zinc. **F. Expression from promoter of *ravvia*** was measured using fluorescent transcriptional fusion of *gfp* expressed from *ravvia* promoter, and quantified using flow cytometry. The Y-axis represents the relative fluorescence in the indicated conditions. Zn: zinc 1.5 mM. NT: non-treated. Δ zur: zur deletion strain. WT: wild type strain. For statistical significance calculations, we used one-way ANOVA. **** means p<0.0001, *** means p<0.001, ** means p<0.01, * means p<0.05. ns: non-significant. Number of replicates for each experiment: 3<n<6.

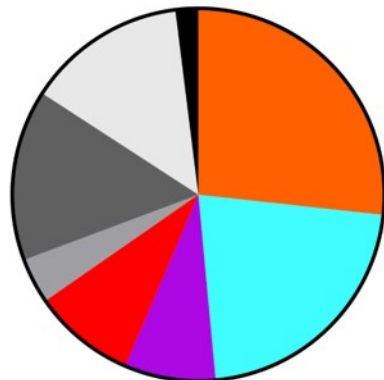
Figure 6: Low ROS phenotype of Δ *ravvia* is dependent on the presence of Cpx and Zra-like stress response systems. Quantification of variation of reactive oxygen species using CellRox. The y-axis represents log₂ fold-change of detected ROS fluorescence in the indicated strain over the WT strain. Each experiment was performed at least 3 times and data and statistical significance are shown in the histograms. For statistical significance calculations, we used one-way ANOVA. **** means p<0.0001, ** means p<0.01. ns means non-significant.

Figure 7: Response of Δ *ravvia* to the membrane targeting antibiotics. A. Minimum inhibitory concentration of vancomycin. MIC values are represented in the Y-axis for the indicated strains. **B.** Outer membrane permeability to nitrocefin measured on stationary phase cultures diluted to 5×10^7 cells/ml by measuring the OD at 490 nm for 40 min. **C.** AG uptake quantified through Neo-cy5 entry into exponential phase cultures. Intracellular level of neomycin coupled to the fluorophore Cy5 measured by fluorescence associated flow cytometry. Error bars represent standard deviation. For statistical significance calculations, we used one-way ANOVA. **** means p<0.0001. Only significant p values are shown.



A**B****C**

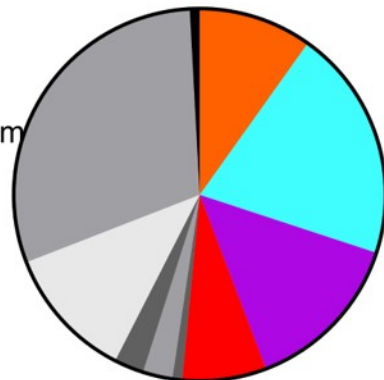
**RNA-seq differential FC>2
Up or down**



Total=101

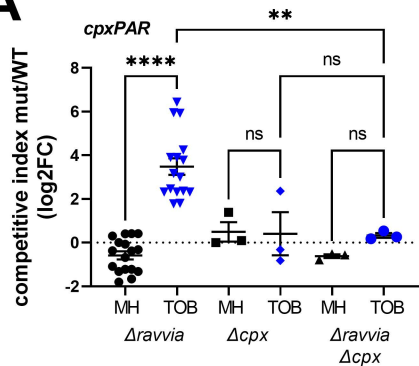
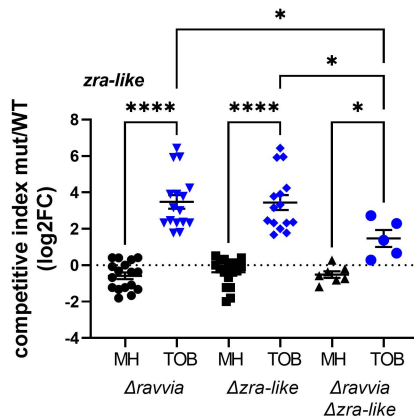
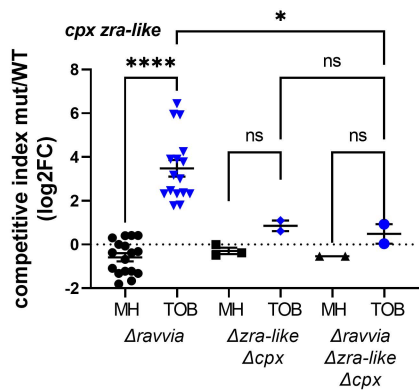
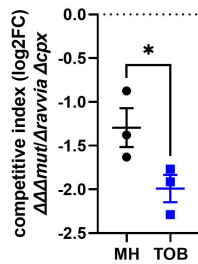
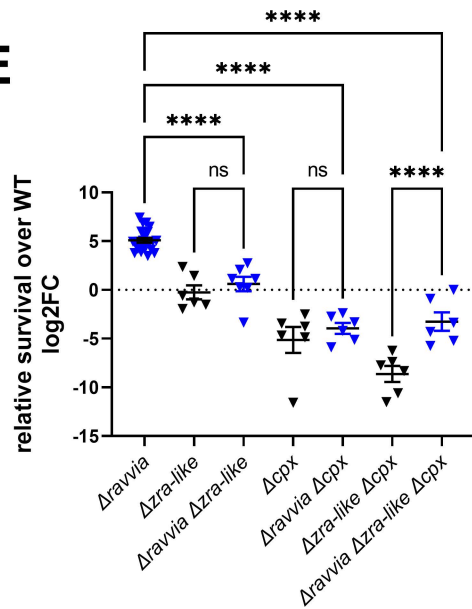
- Carbohydrate metabolism
- Respiration (anaerobic)
- Envelope
- Translation/amino-acid metabolism
- Nucleotide metabolism
- others
- unknown
- quorum sensing

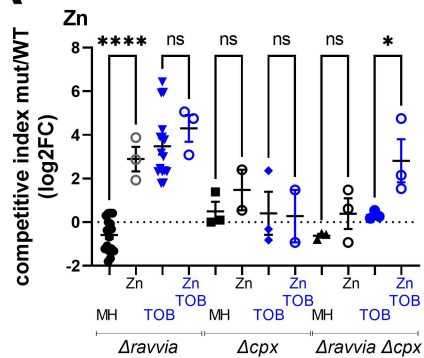
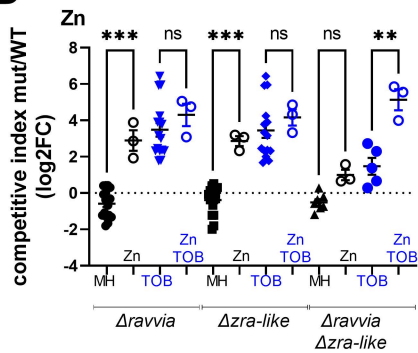
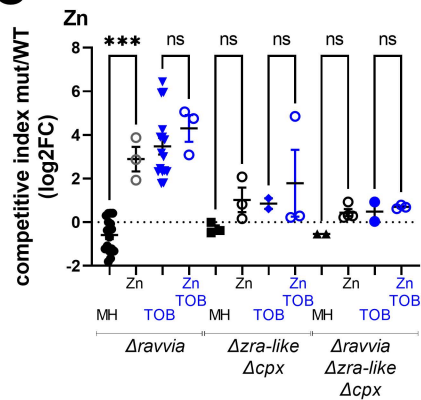
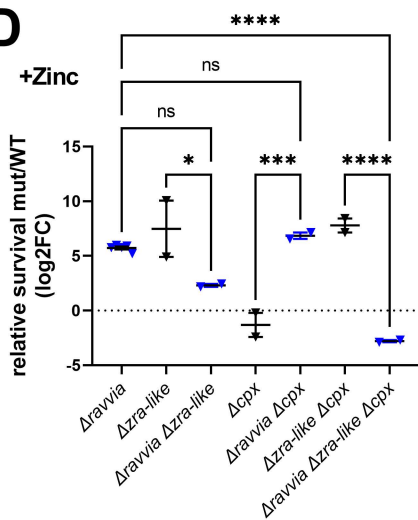
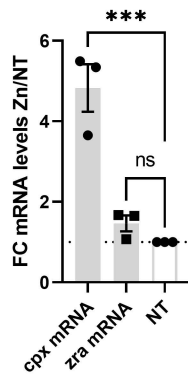
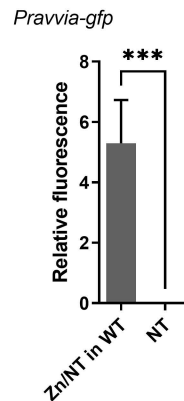
**TN-seq differential FC>2
All conditions**

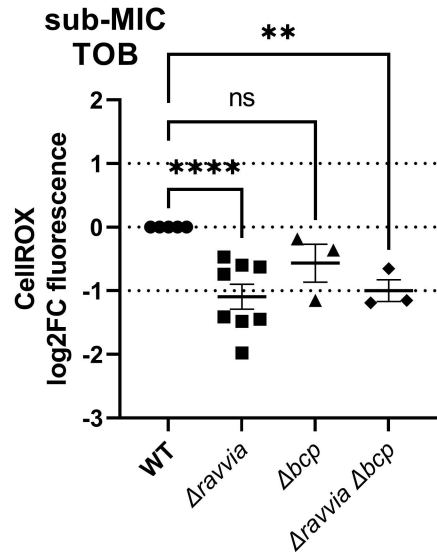
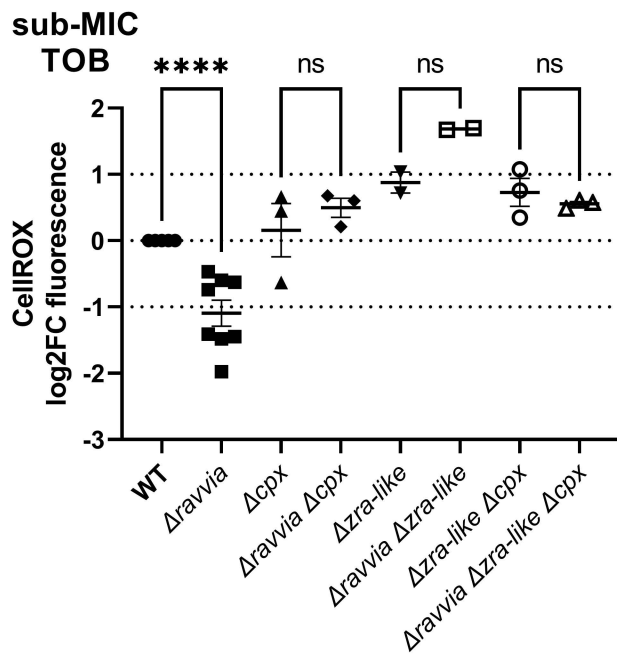
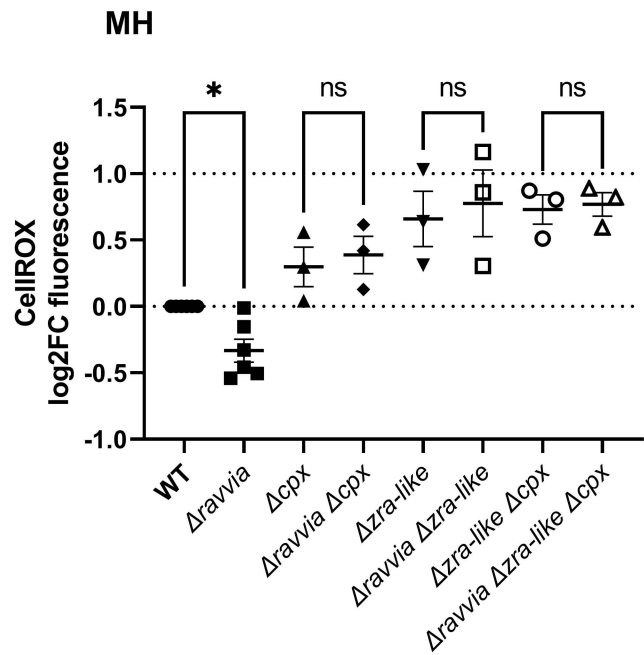


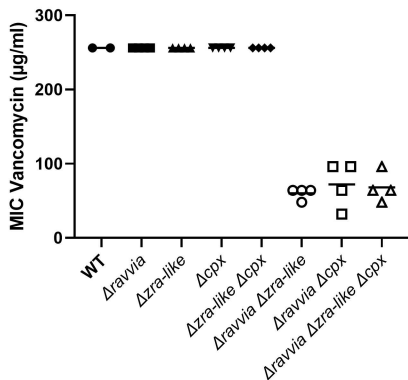
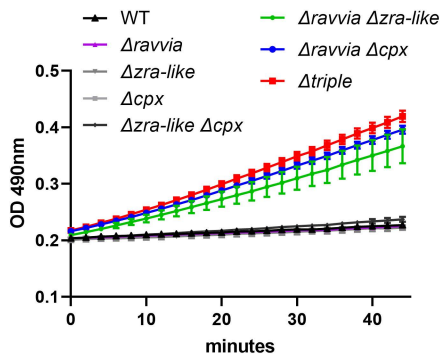
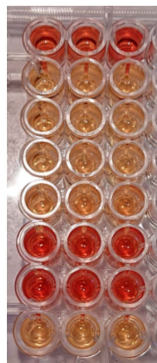
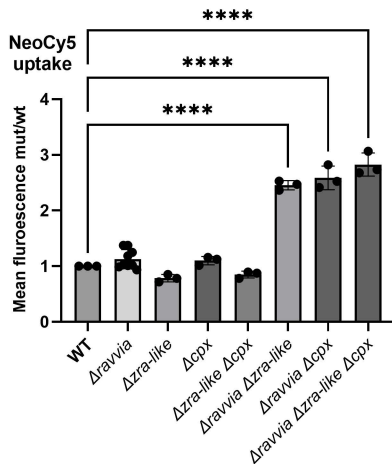
Total=233

- Carbohydrate metabolism
- Fe-S/respiration
- Envelope
- Translation/Protein stress
- Other stress responses
- Flagella
- Others
- Unknown
- quorum sensing
- Nucleotide metabolism

A**B****C****D****E**

A**B****C****D****E****F**



A**B****C**

$\Delta\text{ravvia } \Delta\text{zra-like}$
 Δcpx
 Δravvia
 $\Delta\text{zra-like}$
 $\Delta\text{cpx } \Delta\text{zra-like}$
 $\Delta\text{ravvia } \Delta\text{cpx}$
 triple mutant
 WT

Supplementary figures

Figure S1

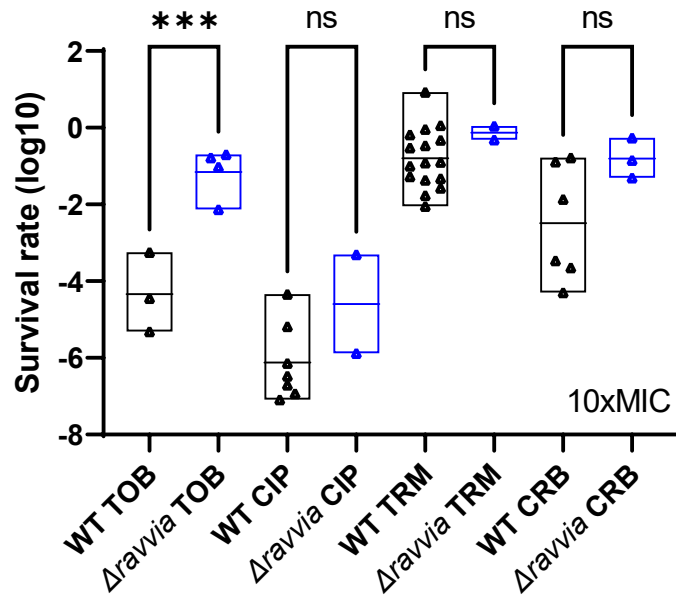


Figure S1: Effect of RavA-ViaA on tolerance to antibiotics. A. Survival of WT and $\Delta ravvia$ to treatment with antibiotics at 10x the MIC. Cultures were grown without antibiotics up to early exponential phase, and treated with antibiotics at lethal concentrations. TOB: tobramycin 10 $\mu\text{g/ml}$. Non-aminoglycoside antibiotics: CIP: ciprofloxacin. TRM: trimethoprim. CRB: carbenicillin. For statistical significance calculations, we used one-way ANOVA. *** means $p < 0.001$, ns means non-significant. Number of replicates for each experiment: $n \geq 3$.

Figure S2. Impact of selected gene deletions in WT and *Δravvia* on fitness during growth in sub-MIC antibiotics: *in vitro* competition experiments of *V. cholerae* WT and mutant strains in the absence or presence of TOB at sub-MICs (50% of the MIC). We were looking for factors for which inactivation would lead to loss of the fitness advantage of *Δravvia* in AGs. We tested the effect of 21 gene deletions, selected because they are important in WT but not in *Δravvia* (panel with red square), important in *Δravvia* (green panel) or beneficial in WT only (purple panel). For 16 of them, none completely suppressed this phenotype. TN-seq screen identified functions that are necessary for AG resistance in *Δravvia*. (i) in the absence of TOB: several genes are no longer essential or as important in *Δravvia* as in WT. These genes include carbohydrate utilization and metabolism genes (*crp*), iron and respiration related factors (*feoC*, *iscX*, *trxC*), and envelope related genes (*cpxP*). This suggests that deletion of *ravvia* leads to changes in carbon metabolism, iron and respiration, and membrane stress. This is consistent with transcriptomic data. Several genes become essential or important in *Δravvia*: genes involved in respiration and iron utilization (e.g. *rdx*, *bcp*); carbohydrate metabolism (*crr*), translation (*truC*, *rluE*) and protein stress (*groES2*, *clpS*, not tested here in competition). (ii) after growth with TOB: several genes are no longer needed in *Δravvia*: electron transport/redox, carbohydrate metabolism (*sgrR*), stringent response and translation stress (e.g. *raiA*, *hpf*, not tested here), envelope and cell division, e.g. *cspE*, coding for a cold shock transcription anti-terminator which interacts specifically with mRNAs that encode membrane proteins [32]. In summary, several functions appear to be less needed in *Δravvia*: proteins protecting ribosomes upon translation stress (e.g. hibernation factors), consistent with the that AGs cause less translation stress in *Δravvia*. For cytochromes, their inactivation probably decreases PMF and confers AG resistance in WT but since *Δravvia* is already more resistant, their effect on PMF may have little impact on AG tolerance of *Δravvia*. Notable phenotypes were conferred by deletion of the *tat* operon (export of folded proteins to the periplasm) which leads to loss of *Δravvia*'s growth advantage in TOB, as well as RNA modification factors *dusB*, *rluB*, *rluE*, for which deletion is known to be beneficial in TOB [18], and *cpxP* which confers an advantage only to the WT strain. MH: no antibiotic treatment (black dots). TOB: tobramycin 0.6 μg/ml (blue dots). The Y-axis represents log₂ of competitive index value calculated as described in the methods. A competitive index of 1 (i.e. log₂ value of 0) indicates equal growth of both strains. Statistical comparisons are between the competition [*Δgene* vs WT] and [*Δgene Δravvia* vs WT]. For statistical significance calculations, we used one-way ANOVA. **** means p<0.0001, *** means p<0.001, ** means p<0.01, * means p<0.05. ns: non-significant. Number of replicates for each experiment: 3<n<6.

Figure S3

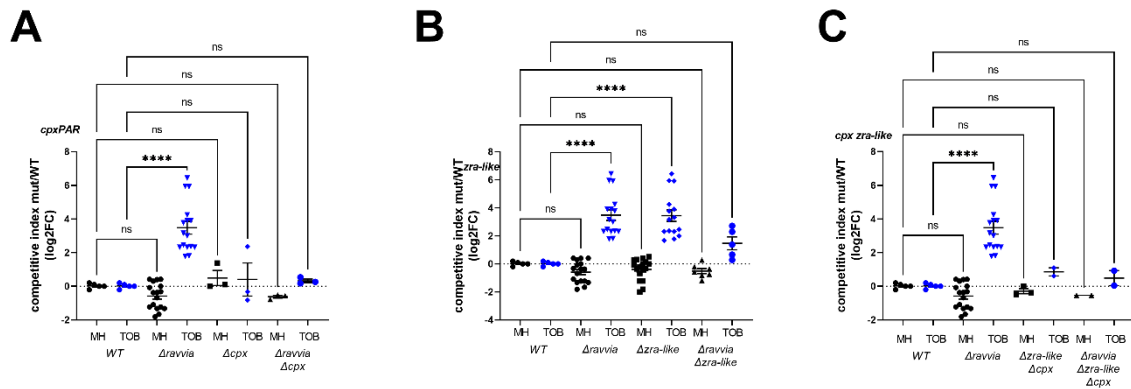


Figure S3. Cpx and Zra-like two component envelope stress response systems are involved in fitness increase of Δ *ravvia* with TOB and TOB tolerance. ABC. Competitions. The effect of deletion of *cpx* (A), or *zra-like* (B), or both (C) on competitive index in MH without and with TOB, where MH is the untreated growth medium. *In vitro* competition experiments of *V. cholerae* WT and indicated mutants in specified media: in black: MH: no antibiotic treatment. In blue: TOB: tobramycin 0,6 μg/ml. The Y-axis represents log₂ of competitive index value calculated as described in the methods. A competitive index of 1 (i.e. log₂ value of 0) indicates equal growth of both strains. Statistical significance compared to WT is shown. The data is the same as in Figure 4. **** means p<0.0001, *** means p<0.001, ** means p<0.01, * means p<0.05. ns: non-significant. Number of replicates for each experiment: 3<n<8.

Figure S4

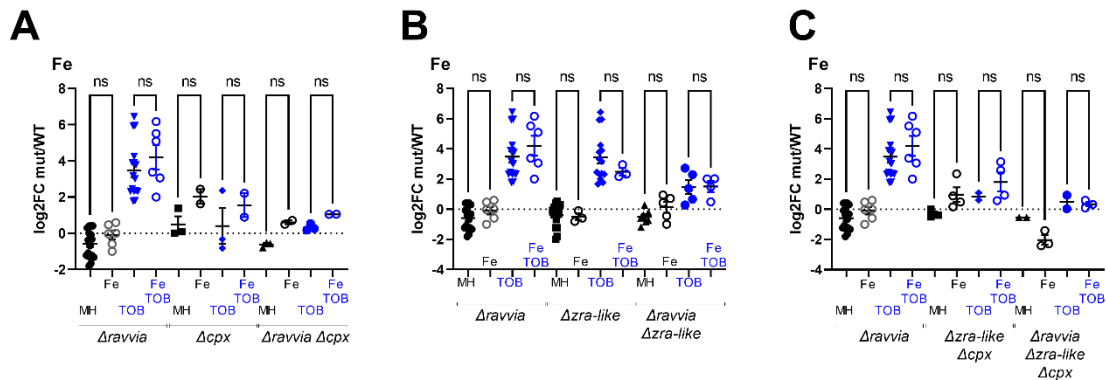


Figure S4: Effect of iron supplementation. ABC. Competitions. The effect of deletion of *cpx* (A), or *zra-like* (B), or both (C) on competitive index in MH with addition of iron, without and with TOB. Cultures were grown to exponential phase in MH medium supplemented with iron during growth. “Fe” stands for FeSO₄ 18μM. *In vitro* competition experiments of *V. cholerae* WT and indicated mutants in specified media: in black: MH: no antibiotic treatment. In blue: TOB: tobramycin 0,6 μg/ml. The Y-axis represents log₂ of competitive index value calculated as described in the methods. A competitive index of 1 (i.e. log₂ value of 0) indicates equal growth of both strains. For statistical significance calculations, we used one-way ANOVA. **** means p<0.0001, *** means p<0.001, ** means p<0.01, * means p<0.05. ns: non-significant. Number of replicates for each experiment: 3<n<8.

Figure S5

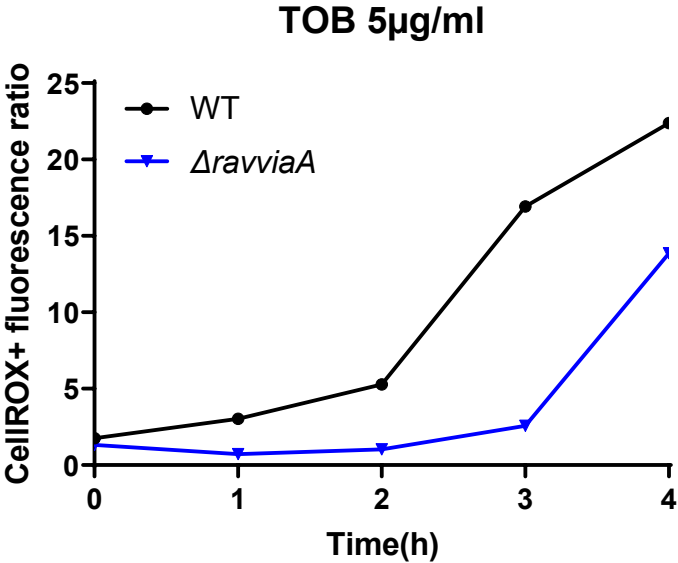


Figure S5: Low ROS phenotype of $\Delta ravvia$ is maintained in the presence of 5x MIC TOB. Quantification of variation of reactive oxygen species using CellRox. The y-axis represents fluorescence corresponding to detected ROS in the indicated strain, as a function of time. Experimental conditions were that of survival assays performed on exponentially growing cultures. Fluorescence was measured using flow cytometry every hour during TOB treatment, on 50,000 cells.

Table S1. RNA-seq

Locus tag	gene name	Fold change* increase in <i>Δravvia</i>
Carbohydrate metabolism		
VC_1820	putative PTS system, mannose specific IIA subunit	104.7
VC_1821	putative PTS system, maltose/mannose-specific IIBC component	11.5
VC_1822	putative PTS system mannose-specific IIA/IIB/IIC components	3.8
VC_1825	Putative ARAC-type regulatory mannose dependent	8.8
VC_1826	<i>manP</i>	27.4
VC_1827	<i>manA</i>	9.9
VC_1325	<i>mglB</i>	16.9
VC_1327	<i>mglA</i>	11.1
VC_A0516	<i>fruA</i>	10.4
VC_A0517	<i>pfkB</i>	10.7
VC_A0518	<i>fruB</i>	9.2
VC_0687	<i>cstA</i>	10.6
VC_A0137	<i>glpT</i>	14.0
VC_A0747	<i>glpA</i>	3.7
VC_A0749	<i>glpC</i>	3.4
VC_1596	<i>gal</i>	7.8
VC_1595	<i>galK</i>	9.8
VC_1594	<i>galM</i>	9.3
VC_1898	<i>trg</i>	4.7
VC_1298	<i>trg</i>	4.0
VC_A1069	<i>tar</i>	4.6
VC_A0903		3.2
VC_2337	<i>galR</i>	3.2
VC_1645		3.1
VC_A0860	<i>malS</i>	3.0
VC_A1041		2.5
VC_A1045		2.2
Aminoacid/protein metabolism		
VC_1343	<i>pepT</i>	11.5
VC_0282	<i>tsr</i>	4.4
VC_0027	<i>ilvA</i>	3.9
VC_1872	<i>yeaG</i>	2.7
VC_A0574	<i>patZ</i>	2.7
VC_2374	<i>gltD</i>	2.5
VC_A0985	<i>htpG</i>	3.3
VC_A0885	<i>tdh</i>	2.4

VC_0392		2.0
Envelope		
*VC_1315	<i>zraS-like</i>	11.4
*VC_1316	<i>zraR/cpxR-like</i>	10.9
VC_1314		8.8
VC_A0867	<i>ompW</i>	5.9
VC_0972	<i>chiP</i>	4.6
VC_1081	<i>ntrC</i>	3.1
VC_1122		2.2
VC_1522	<i>atoC</i>	2.1
Respiration/redox		
*VC_2656	<i>frdA</i>	6.1
*VC_2657	<i>frdB</i>	10.7
*VC_2658	<i>frdC</i>	9.9
*VC_2659	<i>frdD</i>	9.6
VC_1950	<i>torZ</i>	9.9
VC_0651	<i>ubiV</i>	6.7
VC_1951	<i>torY</i>	6.1
VC_A0983	<i>lldP</i>	6.0
VC_A0984	<i>lldD</i>	4.1
VC_A0665	<i>dcuC</i>	5.4
VC_A0205	<i>dcuB</i>	5.1
VC_0338		5.1
VC_A0784		4.6
VC_A0610	<i>elbB</i>	4.3
VC_A0691		4.2
VC_A0512	<i>nrdG</i>	3.6
VC_A0690		3.5
VC_1514	<i>tatB</i>	2.9
VC_1512	<i>ynfG</i>	2.8
VC_1515	<i>torD</i>	2.5
VC_1511		2.4
VC_1516		2.3
Nucleotide metabolism		
VC_A0053		3.3
VC_A0592		3.1
VC_A0798	<i>yieH</i>	2.9
VC_1034	<i>udp</i>	2.6
Others		
VC_2361	<i>grcA</i>	6.6
VC_0076	<i>uspA</i>	4.1
VC_A0904	<i>gntP</i>	3.5
VC_A1015		3.3
VC_0737	<i>acuB</i>	2.9
VC_1605a		2.9

VC_A0689		2.7
VC_0728	<i>ppk2</i>	2.7
VC_A0221		2.6
VC_A0274		2.5
VC_A0688	<i>phaC</i>	2.4
VC_0551		2.3
VC_0550	<i>oadA</i>	2.3
VC_2507	<i>ybeZ</i>	2.1
VC_2473	<i>ytfK</i>	3.8
Quorum Sensing, Competence		
VC_A0865	<i>hapA</i>	2.4
VC_1153	<i>tfoX</i>	4.2
Hypotetical proteins		
VC_A1065		4.7
VC_1080		3.9
VC_0957	<i>ybeL</i>	3.6
VC_A0619		3.0
VC_1690		2.8
VC_2470		2.5
VC_1710		2.2
VC_1698		2.2
VC_A0971		2.1
VC_A0330		2.1
VC_1125		2.1
VC_A0381		2.1
VC_1697		2.0
VC_2221		12.8
Locus tag	gene name	Fold change* decrease in <i>Δravvia</i>
Controls		
VC_A0763	<i>ravA</i>	250
VC_A0762	<i>viaA</i>	142.9
Purine biosynthesis		
VC_2227	<i>purN</i>	3.6
VC_2226	<i>purM</i>	3.4
VC_1004	<i>purF</i>	2.5
Translation, tRNA synthesis		
VC_2706	<i>yhhQ</i>	3.5
VC_1942	<i>folD</i>	2.8
VC_0327	<i>rplL</i>	2.2
VC_0564	<i>rplS</i>	1.9
VC_0325	<i>rplA</i>	1.9
VC_1259	<i>trhO</i>	2.7
VC_t017	<i>tRNA-Thr</i>	2.1
VC_A1059	<i>trmY</i>	2
VC_0916	<i>etp</i>	2.7

Aminoacid transport and synthesis		
VC_0907	<i>metN</i>	2.1
VC_1312	<i>alr</i>	2.1
VC_1658	<i>sdaC</i>	3.3
VC_A0063	<i>ptrB</i>	3.1
Iron-sulfur and respiration		
VC_0538	<i>cysP</i>	2.5
VC_0384	<i>cysJ</i>	2.4
VC_A0064	<i>tonB</i>	2.3
VC_0749	<i>iscU</i>	2
VC_1623	<i>nspC</i>	2.1
VC_1624		2.4
VC_A0779	<i>puuB</i>	2.4
Others		
VC_2561	<i>cobA</i>	2.8
VC_1040	<i>cobO</i>	2.3
VC_1112	<i>bioB</i>	2.6
VC_A0035		2.1

***: only values with adjusted pvalue<0.01 are shown**

Table S2. Transposon insertion sequencing at time T0: genes that cannot be inactivated only in WT or only in *Δravvia*

Non-treated – No insertion detected in WT (no reads) but inactivation possible in <i>Δravvia</i>	
Carbohydrate metabolism	
<i>csrA</i>	Carbon storage regulator, stringent response
<i>bax (VC_1430)</i>	Sugar metabolism (glycoside hydrolase)
<i>crp*</i>	Carbon catabolite control (enriched in <i>ravvia</i> but still very low)
Iron	
<i>yggX (VC_0451)</i>	Role in Fe-S cluster stability, redox sensitive
<i>feoC*(VC_2076)</i>	Ferrous iron uptake, redox sensitive FE-S cluster, Fur regulation
<i>iscX*</i>	Regulator of Fe-S assembly, function unclear
Redox/respiration	
<i>trxC*</i>	Thioredoxin, redox sensitive
<i>dsbD (VC_A0325)</i>	Respiration, thiol:disulfide interchange protein
<i>ubiG (VC_1262)</i>	Respiration, 3-demethylubiquinone-9 3-methyltransferase
Envelope	
<i>cpXP*(VC_2691)</i>	Resistance to extracytoplasmic stress, envelope stress (with degP)
<i>rffM (VC_0927)</i>	Enterobacterial common antigen
<i>tatB*</i> (Export of folded proteins
Others	
<i>ligA VC_1542)</i>	DNA ligase
<i>gspS2</i> (Lipoprotein
<i>higB-1 (VC_A0391)</i>	Toxin
Unknown	
<i>yggU</i>	VC_0458
<i>yhbS</i>	VC_0655
<i>hyp</i>	VC_1613
<i>hyp</i>	VC_1637
<i>hyp</i>	VC_A0381
<i>pseudogene</i>	VC_A0390
<i>hyp</i>	VC_A0467
<i>hyp</i>	VC_A0471
<i>hyp</i>	VC_A0547
<i>hyp</i>	VC_A1030
<i>hyp</i>	VC_0868
Non-treated – No insertion detected in <i>Δravvia</i> (no reads) but inactivation possible in WT	
Expected control genes	
<i>lacZ</i>	No reads in <i>Δravvia</i> because the strain is <i>ΔlacZ</i>
<i>viaA</i>	
<i>ravA</i>	
Redox/respiration/iron	
<i>napC VC_A0680</i>	Cytochrome c
<i>doxX VC_A1019</i>	Oxydoreductase
<i>rdx* VC_0982</i>	Oxidoreductase (selenoprotein W-related protein/selT motif)

<i>grx4</i> VC_2044	Glutaredoxin
<i>bcp*</i> VC_2160	Thioredoxin-Dependent Thiol Peroxidase (homol. to selU YbbB tRNA 2-selenouridine synthase)
VC_0382	Putative ABC-type Fe ³⁺ -hydroxamate transport system
Carbohydrate metabolism	
<i>crr*</i>	Phosphotransfer protein in sugar uptake, regulates sugar metabolism
<i>ace</i>	Isocitrate lyase (deletion =>carbon catabolite repression)
<i>creA*</i> VC_A0800	Catabolite regulation protein
Translation/protein stress	
<i>rrf_9</i> VC_r022	5S Ribosomal RNA, polar on tRNA glu/lys/val
<i>epmC</i> VC_2113	efp hydroxylase
<i>truC</i>	tRNA pseudouridine65 synthase (ile, asp)
<i>rluE*</i>	23S rRNA pseudouridine2457 synthase, P center of the ribosome, associated to AG resistance
<i>clpS</i>	protease
<i>groES2</i> VC_A0819	chaperone
Stress	
<i>crl</i>	stat phase/stress regulator (rpoS regulon)
VC1615	UTP pyrophosphatase, prevent unspecific incorporation of modified bases into RNAs
<i>ytfK</i> VC_2473	Stringent response
Others	
<i>flgJ</i>	peptidoglycan hydrolase , creates holes in the peptidoglycan layer for flagella assembly
VC_0246	LPS transport system permease protein
<i>trpR</i>	tryptophan (trp) transcriptional repressor
Unknown:	
VC_0124	putative lipoprotein L
VC_1176	Trp operon leader peptide TrpL
VC_1537	putative Lipoprotein NlpC
VC_2040	hypothetical
VC_2147	hypothetical
VC_A0233	hypothetical
VC_A0348	Toxin RelE
VC_A0435	hypothetical
VC_A0497	Toxin DhiT
VC_A0652	hypothetical
VC_A0831	hypothetical
VC_A0966	hypothetical
VC_A1061	hypothetical

Table S3. Transposon insertion sequencing at time T16, with no treatment: genes that tolerate more insertions either in WT or in *Δravvia*

Non- treated 16 gen– More insertions in ravvia										
gene name		T0 ravvia	T16 ravvia	T16 TOB ravvia	T0 WT	T16 WT	T16 TOB WT	FC T0 ravvia/wt	FC T16 * ravvia/wt	FC T16 TOB ravvia/wt
carbohydrate metabolism										
<i>araD</i>	VC_A0244	194	174	143	58	110	97	3.3	1.6	1.5
<i>malK</i>		510	242	352	140	96	142	3.6	2.5	2.5
	VC_0549	482	232	334	152	222	173	3.2	1.0	1.9
redox										
	VC_A0506	234	88	212	69	165	108	3.4	0.5	2.0
nucleotide pool										
<i>surE/umpG</i>		409	352	323	140	152	69	2.9	2.3	4.7
<i>pnpP</i>	VC_A0970	331	212	204	91	241	132	3.6	0.9	1.5
envelope/membrane										
	VC_A0152	410	422	344	112	320	150	3.7	1.3	2.3
<i>mshF</i>	VC_0407	869	525	618	154	127	151	5.6	4.1	4.1
<i>vpsQ</i>	VC_0939	901	679	783	292	313	283	3.1	2.2	2.8
others										
<i>mobA</i>		212	141	151	63	67	71	3.4	2.1	2.1
<i>citX</i>		411	331	311	117	203	86	3.5	1.6	3.6
<i>trpD</i>		149	142	187	63	60	59	2.4	2.3	3.2
<i>phhB</i>	VC_A0827	546	391	384	154	178	148	3.5	2.2	2.6
unknown										
<i>alpA</i>	VC_1809	286	373	383	90	112	183	3.2	3.3	2.1
<i>yebG</i>	VC_2326	340	237	286	107	156	110	3.2	1.5	2.6
<i>ynjD</i>	VC_1666	206	225	222	32	98	101	6.3	2.3	2.2
<i>hyp</i>	VC_A0743	259	241	258	50	81	67	5.2	3.0	3.9
<i>hyp</i>	VC_A0440	353	355	421	78	139	69	4.5	2.6	6.1
<i>yaeP</i>	VC_0872	395	348	271	91	184	201	4.3	1.9	1.3
<i>hyp</i>	VC_A0086	297	271	267	71	254	191	4.2	1.1	1.4
<i>hyp</i>	VC_A0649	360	331	318	93	188	195	3.9	1.8	1.6
<i>hyp</i>	VC_A0032	516	417	542	137	158	114	3.8	2.6	4.8
?	VC_A0429-30	195	262	375	52	113	149	3.7	2.3	2.5
<i>hyp</i>	VC_A1030	173	137	115	55	40	58	3.1	3.5	2.0
<i>yecM</i>	VC_2073	191	205	181	61	134	120	3.1	1.5	1.5
Non treated 16 gen– more insertions in WT										
gene name		T0 ravvia	T16 ravvia	T16 TOB ravvia	T0 WT	T16 WT	T16 TOB WT	FC T0 wt/ravvia	FC T16* wt/ravvia	FC T16 TOB wt/ravvia
Translation/protein										
<i>yjgA</i>	VC_2536	51	96	77	163	172	142	3.2	1.8	1.8
membrane transport										
	VC_1605a	16	31	38	198	146	99	12.5	4.7	2.6

<i>pspG</i>		56	194	113	561	579	421	10.0	3.0	3.7
		38	6	25	148	22	27	3.9	3.4	1.1
<i>yhdZ</i>	VC_A1037	55	93	128	177	165	165	3.2	1.8	1.3
carbohydrate metabolism										
<i>pfkA</i>		31	13	28	124	54	62	4.0	4.0	2.2
<i>galU</i>		68	48	23	215	100	16	3.2	2.1	0.7
regulators										
<i>cspA</i>	VC_A0166	30	24	28	115	162	32	3.8	6.7	1.1
<i>marR</i>	VC_A1005	37	92	65	181	190	110	4.8	2.1	1.7
	VC_A0999	65	65	69	239	144	123	3.7	2.2	1.8
FE-S/redox										
<i>dsbD</i>	VC_A0389	39	99	101	155	195	103	4.0	2.0	1.0
<i>ibaG</i>	VC_2515	8	19	9	114	91	6	14.3	4.8	0.7
<i>grxB</i>		36	43	47	129	119	68	3.6	2.7	1.5
	VC_1254	61	102	190	216	193	387	3.5	1.9	2.0
<i>hutC</i>		55	72	88	187	164	127	3.4	2.3	1.4
<i>speB</i>		26	41	19	109	73	35	4.2	1.8	1.9
<i>thiS</i>		63	38	78	202	157	105	3.2	4.1	1.3
electron transfer										
<i>ccmF</i>	VC_A0368	88	136	103	311	224	201	3.5	1.6	2.0
<i>ccmE</i>		61	36	81	190	108	846	3.1	3.0	10.4
<i>cobO</i>		73	77	82	221	180	165	3.0	2.3	2.0
DNA repair										
<i>xthA</i>		37	38	37	140	158	141	3.8	4.1	3.8
two component system										
<i>dpiB citA*</i>	VC_0791	48	67	65	179	161	119	3.7	2.4	1.8
<i>cheY</i>	VC_A1096	61	39	62	207	154	36	3.4	4.0	0.6
others										
<i>hfq</i>		33	38	0	117	116	0	3.5	3.1	no reads
unknown										
<i>hyp</i>	VC_2367	22	103	85	199	173	160	9.0	1.7	1.9
<i>yacL</i>	VC_0605	59	125	131	437	371	224	7.5	3.0	1.7
<i>hyp</i>	VC_A0494	24	35	14	113	141	139	4.8	4.0	10.2
<i>hyp</i>	VC_A0919	60	107	68	284	174	260	4.7	1.6	3.8
<i>ybhG</i>	VC_1659	33	78	73	143	154	104	4.3	2.0	1.4
<i>hyp</i>	VC_A0458	92	127	126	369	275	183	4.0	2.2	1.5
<i>fliT</i>		75	390	89	296	869	23	4.0	2.2	0.3
<i>hyp</i>	VC_2046	143	202	153	539	562	281	3.8	2.8	1.8
<i>hyp</i>	VC_A0387	145	172	183	545	363	288	3.7	2.1	1.6
<i>rstA2</i>	VC_1463	68	17	0	253	205	138	3.7	11.7	no reads in ravvia
<i>wbeT rfbT</i>	VC_0258	37	46	36	136	154	93	3.7	3.3	2.5
<i>unfA</i>	VC_1191	48	81	125	176	128	78	3.6	1.6	0.6
<i>hyp</i>	VC_A1024	136	227	217	483	597	369	3.6	2.6	1.7
<i>hyp</i>	VC_0491	39	81	68	138	123	90	3.5	1.5	1.3

hyp	VC_A0342	59	112	125	189	133	113	3.2	1.2	0.9
-----	----------	----	-----	-----	-----	-----	-----	-----	-----	-----

***: FC T16, only values with adjusted pvalue<0.01 are shown**

Table S4. Transposon insertion sequencing at time T16, with sub-MIC TOB: genes that tolerate more insertions either in WT or in *Δravvia*

gene name	T0 ravvia	T16 ravvia	T16 TOB ravvia	T0 WT	T16 WT	T16 TOB WT	fold decr ease ravvia T16T OB/T 0	fold decr ease WT T16T OB/T 0	FC T16 TOB ravvia a/wt **	
TOB 16gen: insertions decrease in wt but unchanged (or increased) in ravvia => factors needed in TOB in WT but not needed in <i>Δravvia</i>										
electron transport/redox										
<i>VC_A0186</i>	22	92	138	44	60	21	0.7	2.9	6.7	NADH:ubiquinone oxidoreductase subunit 2
<i>VC_A0463</i>	76	177	128	39	89	39	1.4	2.3	3.3	glyoxalase
<i>ahpC</i>	219	221	174	179	107	17	1.3	6.2	10.1	peroxiredoxin C
<i>ypjD</i>	289	300	246	243	203	71	1.2	2.9	3.5	cytochrome c assembly ypjD
<i>ridA</i>	217	145	154	267	191	21	0.9	9	7.2	RidA family redox-regulated chaperone
<i>ubiG</i>	120	153	146	187	172	41	1	4.2	3.5	
<i>potD</i>	470	425	314	249	266	82	1.4	3.2	3.8	spermidine preferential ABC transporter
<i>dksA</i>	117	299	233	111	310	31	1.3	10	7.5	
<i>thiD</i>	200	178	217	89	136	64	0.8	2.1	3.4	
<i>trpB</i>	164	137	131	94	84	18	1	4.5	7.1	
Translation										
<i>raiA</i>	103	101	156	124	52	17	0.6	3.1	9.2	ribosome protection
<i>yeiP</i>	214	208	211	277	271	50	1	5.4	4.2	EFP like protein
<i>hpf</i>	261	170	114	155	81	22	1.5	3.6	5.1	ribosome hibernation
<i>sgrR</i>	212	224	225	119	147	56	1	2.6	4	Sugar transport-related Regulator
envelope/membrane/cell division										
<i>ompR</i>	278	211	167	198	174	40	1.3	4.4	4.2	
<i>envC</i>	357	349	294	271	316	92	1.2	3.4	3.2	murein hydrolase activator (septum)
<i>envZ</i>	393	340	298	310	258	71	1.1	3.6	4.2	
<i>envZ</i>	275	289	161	175	235	47	1.8	5	3.4	sensory histidine kinase
<i>zapD</i>	294	286	282	195	197	75	1	2.6	3.8	
<i>matP</i>	110	215	183	131	139	14	1.2	10	13.2	
<i>ftsE</i>	464	476	331	388	421	63	1.4	6.7	5.3	
<i>ftsX</i>	493	477	447	427	470	77	1.1	6.1	5.8	
<i>DedD</i>	146	298	178	76	173	15	1.7	11.7	12	cell division protein
<i>RlpA</i>	313	335	216	313	306	47	1.6	6.5	4.6	septal ring lytic transglycosylase
<i>YfbV</i>	302	240	210	268	303	30	1.1	9.9	6.9	membrane protein
<i>Blc</i>	372	424	384	195	286	94	1.1	3	4.1	OM lipoprotein
<i>glpG</i>	243	227	176	333	323	33	1.3	9.8	5.3	serine proteases which cleave membrane proteins

<i>cspE*</i>		164	261	135	60	118	1	1.9	185.2	211	cold shock transcription antiterminator interact specifically with mRNAs that encode membrane proteins
<i>nhaB</i>		380	356	279	203	224	76	1.3	2.9	3.7	Na+:H+ antiporter
others											
<i>hapR</i>		397	645	381	295	477	54	1.7	8.9	7.1	Quorum sensing master regulator
<i>menC</i>		376	328	341	178	136	71	1	1.9	4.8	menaquinone synth. (vitK2)
<i>bioD</i>		234	180	135	160	194	37	1.3	5.3	3.7	biotin synth
<i>fkfB</i>		324	379	117	244	165	27	1	4.2	3.2	peptidyl-prolyl cis-trans isomerase
<i>diaA</i>		173	193	202	138	110	59	1	1.9	3.4	DnaA initiator-associating factor for replication initiation
unknown											
<i>yfcl VC_2112</i>		83	126	236	60	43	51	0,4	121.3	4.7	
<i>hyp</i>	VC_1 810	80	134	156	55	109	33	0.5	213.8	4.7	
<i>hyp</i>	VC_A 0003	112	129	203	41	114	60	0.6	206.7	3.4	
<i>hyp</i>	VC_A 0302	183	241	281	190	155	50	0.7	237.9	5.6	
<i>hyp</i>	VC_1 531	160	138	244	62	190	65	0.7	290.4	3.7	
<i>tldD</i>		262	334	358	210	272	87	0.7	372.0	4.1	
<i>plsY</i>		167	144	116	251	173	36	1.4	120.5	3.2	
<i>yhbS</i>	VC_0 655	329	261	275	139	78	32	1.2	65.8	8.5	
	VC_A 0808	118	230	121	212	270	6	1.0	277.6	21.2	
<i>phnX</i>	VC_A 0606	204	238	262	106	108	86	0.8	138.4	3.1	
<i>hyp</i>	VC_1 613	280	357	352	121	111	75	0.8	140.0	4.7	
<i>YeeX</i>	VC_A 0741	168	171	177	84	138	2	0.9	145.7	74.7	
<i>hyp</i>	VC_1 262	143	298	171	77	63	23	0.8	75.5	7.4	
<i>hyp</i>	VC_1 479	313	323	303	171	229	90	1.0	221.3	3.4	
<i>hyp</i>	VC_A 0631	121	167	168	74	86	43	0.7	119.6	3.9	
<i>hyp</i>	VC_2 434	347	294	297	216	176	97	1.2	150.5	3.1	
<i>hyp</i>	VC_1 574	213	219	286	156	151	93	0.7	202.4	3.1	
<i>hyp</i>	VC_1 310	192	149	185	144	151	49	1.0	146.2	3.8	
<i>hyp</i>	VC_A 0382	262	232	251	220	146	75	1.0	140.7	3.4	
	VC_1 536	129	172	192	131	122	52	0.7	182.4	3.7	
	VC_A 0331-2	103	150	119	112	126	22	0.9	146.1	5.5	
TOB 16gen: insertions highly decrease in wt but slightly decreased in ravvia => factors needed in TOB in WT but less needed in Δravvia translation											
<i>miaB*</i>		251	234	119	253	233	39	2	6	3.1	tRNA modification
<i>rsmI</i>		378	299	122	441	297	34	2.4	8.6	3.6	rRNA modification
flagella											
<i>fliR</i>		153	663	314	118	684	73	2.1	9.4	4.3	

<i>flhA</i>	186	798	358	157	773	90	2.2	8.6	4		
<i>fliF</i>	181	729	340	266	994	88	2.1	11.3	3.9		
<i>fliG</i>	119	501	202	202	758	58	2.5	13	3.5		
<i>FlgN</i>	198	639	165	222	571	40	3.9	14.3	4.1	flagella synthesis protein	
<i>flgF</i>	178	594	266	243	885	77	2.2	11.5	3.4		
carbohydrate metabolism											
<i>cpsB</i>	640	1545	498	625	1503	36	3.1	41.8	13.8	mannose-1-phosphate guanylyltransferase	
<i>manB</i>	382	1005	340	437	1006	20	3	50.6	17.1	phosphomannomutase	
<i>wcaJ</i>	163	378	132	269	640	22	2.9	29.3	6	UDP-glucose:undecaprenyl-phosphate glucose-1-phosphate transferase	
<i>manA_1</i>	608	630	299	665	587	30	2.1	19.4	9.9		
<i>gmd</i>	718	1230	131	402	989	38	9.4	25.7	3.4	GDP-mannose 4,6-dehydratase	
envelope/membrane/cell division											
<i>phoB</i>	229	307	145	151	192	23	2.1	8.2	6.2		
<i>mepM</i>	342	373	176	423	315	56	2.1	5.7	3.2	Peptidoglycan-specific endopeptidase	
others											
<i>VC_2654</i>	324	379	117	244	165	27	3.2	6.1	4.3	rhodanese-like domain-containing protein thiosulfate disproportionation	
<i>aspA</i>	251	488	197	358	559	44	2.5	12.7	4.5		
gene name	T0 ravvia	T16 ravvia	T16 TOB ravvia	T0 WT	T16 WT	T16 TOB WT	fold increase ravvia	fold increase WT	FC T16 TOB wt/ravvia	**	
TOB 16gen: insertions increase in wt but unchanged in ravvia => important for Δravvia growth in TOB or inactivation has no additional benefit in Δravvia => partners/linked processes?											
translation/protein stress											
<i>VC_0803</i>	<i>trmH*</i>	130	87	148	221	147	801	1.7	5.5	5.4	tRNA modification
	<i>rluB*</i>	110	60	96	152	111	1049	1.6	9.5	11.0	rRNA modification
	<i>dusB*</i>	183	118	184	116	91	1118	1.6	12.3	6.1	tRNA modification
	<i>slyD</i>	44	48	75	97	108	348	1.6	3.2	4.7	Chaperone
iron											
	<i>hemF</i>	108	95	136	87	104	422	1.4	4	3.1	
	<i>fur*</i>	5	7	7	43	6	157	0.9	26.8	23.1	
electron transport/ Fe-S/redox											
	<i>ccoO</i>	115	75	141	205	47	1405	1.9	29.9	9.9	cytochrome C oxidase
	<i>ccoG</i>	163	81	179	181	124	1938	2.2	15.6	10.8	cytochrome c
	<i>VC_0574</i>	88	51	136	165	112	1613	2.7	14.4	11.9	cytochrome b
	<i>VC_0575</i>	136	37	146	114	53	1432	3.9	27	9.8	cytochrome c
	<i>VC_0168</i>	118	63	165	82	58	1859	2.6	32.1	11.3	cytochrome b
	<i>ccmG</i>	94	61	92	92	28	441	1.5	15.8	4.8	cytochrome c biogenesis protein
	<i>ccmE</i>	61	36	81	190	108	846	2.2	7.8	10.4	cytochrome c
	<i>ccmA</i>	77	47	105	117	60	483	2.2	8.1	4.6	cytochrome c

<i>ccml</i>	59	55	105	109	119	353	1.9	3	3.4	cytochrome c biogenesis	
<i>arcA_2</i>	147	47	57	113	23	289	1.2	12.6	5.1	response regulator, regulates cadA	
<i>arcB</i>	195	64	97	193	41	480	1.5	11.6	4.9	response regulator, regulates cadA	
<i>dsbD</i> <i>dipZ</i>	118	77	146	136	89	686	1.9	7.7	4.7	thiol:disulfide interchange	
<i>ychF</i>	72	21	57	99	58	737	2.7	12.7	12.9	redox-responsive ATPase	
<i>cadA</i> = <i>ldcI</i> *	95	39	115	98	109	1491	2.9	13.7	13.0		
<i>iscR</i> *	21	27	61	47	46	845	2.2	18.4	13.9		
carbohydrate metabolism											
<i>crr</i> *	32	16	14	156	23	489	0.9	21.3	33.9	glucose uptake	
<i>ptsI</i>	74	19	56	99	27	867	3	32.7	15.5		
<i>ptsH</i>	50	41	3	79	78	230	0.1	2.9	86.6	phosphocarrier protein HPr	
<i>pykF</i>	42	16	39	82	32	218	2.4	6.8	5.6	pyruvate kinase	
<i>rpiR</i>	115	64	103	84	32	497	1.6	15.4	4.8	carbohydrate utilization regulator	
<i>rpe</i>	174	32	62	175	39	536	1.9	13.9	8.6	ribulose-phosphate 3-epimerase	
envelope/membrane/motility											
<i>bamC</i>	255	100	174	180	88	555	1.7	6.3	3.2	outer membrane protein assembly	
<i>mioC</i>	175	50	161	113	69	827	3.3	12.1	5.1	flavoprotein, cell division	
<i>VC_1_422</i>	166	148	98	160	143	662	0.7	4.6	6.8	sodium:alanine symporter	
<i>hdfR</i>	73	66	137	137	139	779	2.1	5.6	5.7	negative regulator of flagella	
others											
<i>luxO</i>	126	102	168	146	108	711	1.7	6.6	4.2	QS	
<i>citG</i>	193	191	191	296	283	633	1	2.2	3.3		
unknown											
<i>VC_0_124</i>	98	36	47	180	178	1016	1.3	5.7	21.7	putative lipoprotein L	
<i>VC_2_498</i>	61	34	112	183	126	1508	3.3	12	13.4		
<i>VC_A_0039</i>	72	33	135	130	155	1833	4.1	11.8	13.6	putative cobaltochelate subunit CobN	
YfcZ	<i>VC_A_0919</i>	60	107	68	284	174	260	0.6	1.5	3.8	
ybfF	<i>VC_2_097</i>	100	122	160	201	225	518	1.3	2.3	3.2	
	<i>VC_A_1061</i>	106	64	54	129	261	163	0.8	0.6	3.0	
	<i>VC_2_476</i>	46	67	53	126	189	228	0.8	1.2	4.3	

** : FC T16TOB, only values with adjusted pvalue<0.01 are shown

Table S5.

Strain #	genotype	resistance	parental strain	construction	primers for gibson assembly or details for cloning
J085	<i>WT V. cholerae N16961 hapR+</i>	strep		lab collection	
K329	<i>WT V. cholerae N16961 hapR+ ΔlacZ</i>	strep	J085	laboratory collection	deletion of lacZ by conjugation J085*4850 and sucrose 15% excision
L555	<i>ΔravA-viaA::spec ΔlacZ</i>	spec	K329	pMP7 L571	p9344 digested with EcoRI and cloned into pMP7 EcoRI site
M093	<i>ΔravA-viaA::kan ΔlacZ</i>	f _{rt} ::kan::f _{rt}	K329	pMP7 L911	y _{ei} MN5/7 for up region and y _{ei} MN6/8 for down region
O390	<i>ΔravA-viaA ΔlacZ</i>		M093	excision of f _{rt} ::kan::f _{rt}	
O506	<i>ΔravA-viaA pGBts-ravA-viaA+</i>	spec 30°C		transformation of thermosensitive low copy pGBts plasmid expressing <i>ravvia</i> into <i>ravvia</i> deleted strain.	operon <i>ravA-viaA</i> with its own promoter amplified with primers Pravaviamonteco and Opravaviavaleco and clones inside EcoRI of pGBts
M145	<i>WT::Pbla-ravA-viaA-extracopy OE+</i>	Cm5	J085	tn7 transposition pM060	Pbla-ravA-viaA cloned in Xmal into pMVM4 (=L950)
N542	<i>ΔravA::kan ΔlacZ</i>	f _{rt} ::kan::f _{rt}	K329	pMP7 N624	y _{ei} MN5/7 for up region and y _{ei} N6/8 for down region
N601	<i>ΔravA ΔlacZ</i>	-	N542	excision of f _{rt} ::kan::f _{rt}	
N544	<i>ΔviaA::kan ΔlacZ</i>	f _{rt} ::kan::f _{rt}	K329	pMP7 N625	y _{ei} M5/7 for up region and y _{ei} MN6/8 for down region
N620	<i>ΔviaA ΔlacZ</i>	-	N544	excision of f _{rt} ::kan::f _{rt}	
S490	<i>ΔcpxPAR::kan</i>	f _{rt} ::kan::f _{rt}	K329	pMP7 S448	cpxPAR5/7 for up region and cpxAR6bis/8 for down region
Q080	<i>Δzra2 (ΔVC1315-1316) ΔlacZ</i>	f _{rt} ::kan::f _{rt}	K329	pMP7 P679	VC1315-165/7 for up region and VC1315-166/8 for down region

R292	<i>Δzra2 (ΔVC1315-1316) ΔlacZ</i>	-	Q080	excision of <i>frt::kan::frt</i>	
S492	<i>Δzra2 (ΔVC1315-1316) ΔlacZ ΔcpxPAR::kan</i>	<i>frt::kan::frt</i>	R292	pMP7 S448	cpxPAR5/7 for up region and cpxAR6bis/8 for down region
S565	<i>ΔlacZ ΔravA-viaA ΔcpxPAR::kan</i>	<i>frt::kan::frt</i>	O390	pMP7 S448	cpxPAR5/7 for up region and cpxAR6bis/8 for down region
R496	<i>ΔlacZ ΔravA-viaA Δzra2::kan</i>	<i>frt::kan::frt</i>	O390	pMP7 P679	VC1315-165/7 for up region and VC1315-166/8 for down region
S186	<i>ΔlacZ ΔravA-viaA Δzra2</i>		R496	excision of <i>frt::kan::frt</i>	
S547	<i>ΔravA-viaA ΔcpxPAR::kan Δzra2 ΔlacZ</i>	<i>frt::kan::frt</i>	S186	pMP7 S448	cpxPAR5/7 for up region and cpxAR6bis/8 for down region
P640	<i>ΔlacZ Δbcp::kan</i>	<i>frt::kan::frt</i>	K329	pMP7 O650	VC2160bcp5/7 for up region and VC2160bcp6/8 for down region
P739	<i>ΔravA-viaA Δbcp::kan ΔlacZ</i>	<i>frt::kan::frt</i>	O390	pMP7 O650	VC2160bcp5/7 for up region and VC2160bcp6/8 for down region
Q900	<i>ΔlacZ ΔfrdA-D::kan</i>	<i>frt::kan::frt</i>	K329	pMP7 P358	frdAD5/7 for up region and frdAD6/8 for down region
U239	<i>ΔravA-viaA ΔlacZ ΔfrdA-D::kan</i>	<i>frt::kan::frt</i>	O390	pMP7 P358	frdAD5/7 for up region and frdAD6/8 for down region
Q695	<i>ΔlacZ Δsdh::kan</i>	<i>frt::kan::frt</i>	K329	pMP7 P680	VC2088-91sdh5/7 for up region and VC2088-91sdh6bis/8 for down region
Q079	<i>ΔravA-viaA ΔlacZ Δsdh::kan</i>	<i>frt::kan::frt</i>	O390	pMP7 P680	VC2088-91sdh5/7 for up region and VC2088-91sdh6bis/8 for down region
Q063	<i>ΔlacZ ΔfeoC::kan</i>	<i>frt::kan::frt</i>	K329	pMP7 P347	VC2076feoC5/7 for up region and VC2076feoC6/8 for down region
Q064	<i>ΔravA-viaA ΔlacZ ΔfeoC::kan</i>	<i>frt::kan::frt</i>	O390	pMP7 P347	VC2076feoC5/7 for up region and VC2076feoC6/8 for down region
Q101	<i>ΔlacZ ΔiscX::kan</i>	<i>frt::kan::frt</i>	K329	pMP7 P349	VC0754iscX5/7 for up region and VC0754iscX6/8 for down region

Q066	<i>ΔravA-viaA ΔlacZ ΔiscX::kan</i>	frt::kan::frit	O390	pMP7 P349	VC0754iscX5/7 for up region and VC0754iscX6/8 for down region
Q068	<i>ΔravA-viaA ΔlacZ ΔtrxC::kan</i>	frt::kan::frit	O390	pMP7 P352	VCA0752trxC5/7 for up region and VCA0752trxC6/8 for down region
Q077	<i>ΔlacZ ΔcspE::kan</i>	frt::kan::frit	K329	pMP7 P677	VCA0184capB5/7 for up region and VCA0184capB6/8 for down region
Q078	<i>ΔravA-viaA ΔlacZ ΔcspE::kan</i>	frt::kan::frit	O390	pMP7 P677	VCA0184capB5/7 for up region and VCA0184capB6/8 for down region
L168	<i>ΔlacZ ΔmiaB::kan</i>	frt::kan::frit	K329	pMP7 J744	Negro et al, mBio, 2019
O980	<i>ΔravA-viaA ΔlacZ ΔmiaB::kan</i>	frt::kan::frit	O390	pMP7 J744	Negro et al, mBio, 2019
Q081	<i>ΔlacZ Δcrp::spec</i>	spec	K329	pMP7 8348	Baharoglu et al, J Bact, 2012
Q083	<i>ΔravA-viaA ΔlacZ Δcrp::spec</i>	spec	O390	pMP7 8348	Baharoglu et al, J Bact, 2012
Q070	<i>cpxP::kan ΔlacZ</i>	frt::kan::frit	K329	pMP7 P353	VC2691cpxP5/7 for up region and VC2691cpxP6/8 for down region
Q072	<i>ΔravA-viaA ΔcpxP::kan ΔlacZ</i>	frt::kan::frit	O390	pMP7 P353	VC2691cpxP5/7 for up region and VC2691cpxP6/8 for down region
S384	<i>ΔtatABC::kan ΔlacZ</i>	frt::kan::frit	K329	pMP7 F164	Krin et al, BMC , 2022
T618	<i>ΔravA-viaA ΔtatABC::kan ΔlacZ</i>	frt::kan::frit	O390	pMP7 F164	Krin et al, BMC , 2022
T654	<i>ΔlacZ ΔsgrR::kan</i>	frt::kan::frit	K329	pMP7 P676	VCA0578sgrR5bis/7 for up region and VCA0578sgrR6/8bis for down region
Q076	<i>ΔlacZ ΔravA-viaA ΔsgrR::kan</i>	frt::kan::frit	O390	pMP7 P676	VCA0578sgrR5bis/7 for up region and VCA0578sgrR6/8bis for down region
P645	<i>ΔlacZ Δrdx::kan</i>	frt::kan::frit	K329	pMP7 P331	VC0982rdx5/7 for up region and VC0982rdx6/8 for down region
P736	<i>ΔlacZ ΔravA-viaA Δrdx::kan</i>	frt::kan::frit	O390	pMP7 P331	VC0982rdx5/7 for up region and VC0982rdx6/8 for down region
Q061	<i>ΔlacZ ΔrluE::kan</i>	frt::kan::frit	K329		Babosan et al, microLife, 2022

T608	<i>ΔlacZ ΔravA-viaA ΔrluE::kan</i>	frt::kan::frt	O390	pMP7 P346	Babosan et al, microLife, 2022
P725	<i>ΔlacZ Δcrr::kan</i>	frt::kan::frt	K329	pMP7 P333	VC0964crr5/7 for up region and VC0964crr6/8 for down region
P744	<i>ΔravA-viaA ΔlacZ Δcrr::kan</i>	frt::kan::frt	O390	pMP7 P333	VC0964crr5/7 for up region and VC0964crr6/8 for down region
S388	<i>ΔlacZ ΔdcuA::kan</i>	frt::kan::frt	K329	pMP7 S156	dcuA5/7 for up region and dcuA6/8 for down region
T297	<i>ΔlacZ ΔdcuA</i>		S388	excision of <i>frt::kan::frt</i>	
S405	<i>ΔravA-viaA ΔlacZ ΔdcuA::kan</i>	frt::kan::frt	O390	pMP7 S156	dcuA5/7 for up region and dcuA6/8 for down region
T344	<i>ΔravA-viaA ΔlacZ ΔdcuA</i>		S405	excision of <i>frt::kan::frt</i>	
U352	<i>ΔlacZ ΔdcuB::kan</i>	frt::kan::frt	K329	pMP7 S158	dcuB5/7 for up region and dcuB6/8 for down region
U354	<i>ΔravA-viaA ΔlacZ ΔdcuB::kan</i>	frt::kan::frt	O390	pMP7 S158	dcuB5/7 for up region and dcuB6/8 for down region
U353	<i>ΔlacZ ΔdcuA dcuB::kan</i>	frt::kan::frt	T297	pMP7 S158	dcuB5/7 for up region and dcuB6/8 for down region
U356	<i>ΔravA-viaA ΔlacZ ΔdcuA dcuB::kan</i>	frt::kan::frt	T344	pMP7 S158	dcuB5/7 for up region and dcuB6/8 for down region
L559	<i>ΔlacZ ΔrluB::kan</i>	frt::kan::frt	K329		Babosan et al, microLife, 2022
T612	<i>ΔravA-viaA ΔlacZ ΔrluB::kan</i>	frt::kan::frt	O390	pMP7 L020	Babosan et al, microLife, 2022
L606	<i>ΔlacZ ΔdusB::kan</i>	frt::kan::frt	K329		Babosan et al, microLife, 2022
T614	<i>ΔravA-viaA ΔlacZ ΔdusB::kan</i>	frt::kan::frt	O390	pMP7 L416	Babosan et al, microLife, 2022
N540	<i>Δfur::kan</i>	frt::kan::frt	J085	pMP7 N231	VC2106fur5/7 for up region and VC2106fur9/8 for down region
Q896	<i>ΔravA-viaA ΔlacZ Δfur::kan</i>	frt::kan::frt	O390	pMP7 N231	VC2106fur5/7 for up region and VC2106fur9/8 for down region
Q699	<i>ΔlacZ ΔldcI::kan</i>	frt::kan::frt	K329	pMP7 P338	VC0281ldlcada5/7 for up region and VC0281ldlcada6/8 for down region

Q074	<i>ΔravA-viaA ΔlacZ ΔldcI::kan</i>	frt::kan::frt	O390	pMP7 P338	VC0281ldlcada5/7 for up region and VC0281ldlcada6/8 for down region
Q701	<i>ΔlacZ ΔiscR::kan</i>	frt::kan::frt	K329	pMP7 P355	VC0747iscR5/7 for up region and VC0747iscR6/8 for down region
U426	<i>ΔlacZ ΔiscR</i>		Q701	excision of <i>frt::kan::frt</i>	
Q899	<i>ΔlacZ ΔravA-viaA ΔiscR::kan</i>	frt::kan::frt	O390	pMP7 P355	VC0747iscR5/7 for up region and VC0747iscR6/8 for down region
U493	<i>ΔlacZ ΔravA-viaA ΔiscR</i>		Q899	excision of <i>frt::kan::frt</i>	
Q696	<i>ΔlacZ ΔptsI-H::kan</i>	frt::kan::frt	K329	pMP7 P494	VC0965-6ptsIH5/7 for up region and VCVC0965-6ptsIH6bis/8 for down region
S407	<i>ΔlacZ ΔravA-viaA ΔptsI-H::kan</i>	frt::kan::frt	O390	pMP7 P494	VC0965-6ptsIH5/7 for up region and VCVC0965-6ptsIH6bis/8 for down region
P638	<i>ΔlacZ ΔtruC::kan</i>	frt::kan::frt	K329		Babosan et al, microLife, 2022
P741	<i>ΔlacZ ΔravA-viaA ΔtruC::kan</i>	frt::kan::frt	O390	pMP7 O651	Babosan et al, microLife, 2022

Table S6: Primers

primers	
yeiMN5	CTATTATTTAAACTCTTCCACGACAATCTCGCCTTGGT
yeiMN7	CTACACAATCGCTCAAGACGTGCTCTTGATTCTCAGACAAAG
yeiMN8	CTAATTCCCATGTCAGCCGTCTTGAATGCTTCATACCCAAC
yeiMN6	TACGTAGAATGTATCAGACTATAAAAAACGTCATAAGAATAGC
VC2106fur5	CTATTATTTAAACTCTTCCAAGCGGATGCGAACTTCGC
VC2106fur7	CTACACAATCGCTCAAGACGTGATACTTCTGTTGATGTTCTGC
VC2106fur8	CTAATTCCCATGTCAGCCGTGCTCACAAGCCGAAGAAATAA
VC2106fur9	TACGTAGAATGTATCAGACTCCACAAATCGATCAGTTTATGG
yeiN8	CTAATTCCCATGTCAGCCGTGCATTGTAACCTCAACCAA
yeiN6	TACGTAGAATGTATCAGACTACGCTCTTGTGGCTTTAAG
yeiM5	CTATTATTTAAACTCTTCCCGTTATTGCAGAGCAATATGTC
yeiM7	CTACACAATCGCTCAAGACGTGAATGACACCTAAGCAAAAAATTG
Pravaviamonteco	GGAATTCTATTGAACTATTGTTTATAGAGCG
Opravaviavaleco	GGAATTCTTACCACTTCTTCATTAGCCG
VCA0578sgrR5bis	CTATTATTTAAACTCTTCCGACACGACAATCGCGTTACC
VCA0578sgrR7	CTACACAATCGCTCAAGACGTGAAAGAGGAAATCTCATCTAACTT
VCA0578sgrR8	CTAATTCCCATGTCAGCCGTCTTTACTCACTCGTGGGAT
VCA0578sgrR6bis	TACGTAGAATGTATCAGACTTTGTTCTCTGCCATCTCTTTTTTC
VC0982rdx5	CTATTATTTAAACTCTTCCATATTGGGGGAGTGACTTCA
VC0982rdx7	CTACACAATCGCTCAAGACGTGCGTGACGTCCTTGTATGTC
VC0982rdx8	CTAATTCCCATGTCAGCCGTGCGATCCCCAAACGACTCAG
VC0982rdx6	TACGTAGAATGTATCAGACTAATCCTATCCCGAAGGGTA
VC2160bcp5	CTATTATTTAAACTCTTCCGAAGTGGTTCGATTAGTGAC
VC2160bcp7	CTACACAATCGCTCAAGACGTGAATTATCCCTTTGATTACTGACT
VC2160bcp8	CTAATTCCCATGTCAGCCGTATCGGTAGAAATGCCGATTTT
VC2160bcp6	TACGTAGAATGTATCAGACTGCCGATGAAGTTCGGACGTT
VC0964crr5	CTATTATTTAAACTCTTCCAAGAAGTCTCTTCTCTCTATC
VC0964crr7	CTACACAATCGCTCAAGACGTGTGTCATGCTCCTAACGTT
VC0964crr8	CTAATTCCCATGTCAGCCGTGACCAAGTAATCGCTTGG

VC0964crr6	TACGTAGAATGTATCAGACTATTAAGTGTGCAACACGG
VC0965-6ptsIH5	CTATTATTTAAACTCTTTCAAATGGCGCGTCGCCTAATG
VC0965-6ptsIH7	CTACACAATCGCTCAAGACGTGTTTTATACCCAATGAGTTTA
VC0965-6ptsIH8	CTAATTCCCATGTCAGCCGTTATCGGTTGATACCAAGGA
VC0965-6ptsIH6bis	TACGTAGAATGTATCAGACTCAACGATTTTCTCAGCGAAAA
VC2076feoC5	CTATTATTTAAACTCTTTCCAGCACACCTGATGCAGAAGA
VC2076feoC7	CTACACAATCGCTCAAGACGTGCGACAGATACCTCTATCAT
VC2076feoC8	CTAATTCCCATGTCAGCCGTAACCTTCCAACCTGAAGGTG
VC2076feoC6	TACGTAGAATGTATCAGACTAGCTGGTTTGCCAAACTCTG
VC2691cpxP5	CTATTATTTAAACTCTTTCCGATCGCTAAAAGGTTTGGGC
VC2691cpxP7	CTACACAATCGCTCAAGACGTGCGTTCGTTCTCTACATTC
VC2691cpxP8	CTAATTCCCATGTCAGCCGTCAAAAAACACGCTAGTCAATAA
VC2691cpxP6	TACGTAGAATGTATCAGACTGTTGAGGATCAAAAAGCACG
VC0747iscR5	CTATTATTTAAACTCTTTCCAACGTAAGTGGCTTGACCAAT
VC0747iscR7	CTACACAATCGCTCAAGACGTGAATCACACCGTATCCACACT
VC0747iscR8	CTAATTCCCATGTCAGCCGTCGGCAAGGTTTACACTGGAG
VC0747iscR6	TACGTAGAATGTATCAGACTGCCGATTTTCATTGTTACGCT
VC2088-91sdh5	CTATTATTTAAACTCTTTCTAAAGTACGAACGTCAATCAC
VC2088-91sdh7	CTACACAATCGCTCAAGACGTGTCAGCTCCATTGAGCATTAT
VC2088-91sdh8	CTAATTCCCATGTCAGCCGTACATATTAAGTCCATGTTGATC
VC2088-91sdh6bis	TACGTAGAATGTATCAGACTATTCGTTGGGTGCGCAGGCA
VC0754iscX5	CTATTATTTAAACTCTTTCTATAAAAGACACAGACAAAGCG
VC0754iscX7	CTACACAATCGCTCAAGACGTGGTTAGCCTTCTATTGGTT
VC0754iscX8	CTAATTCCCATGTCAGCCGTTCTCATGCAAAATGAAGTG
VC0754iscX6	TACGTAGAATGTATCAGACTGCCGCTAAAGCTTTCCACTC
VCA0752trxC5	CTATTATTTAAACTCTTTCCGCGTTGAGATCAAAGGCGGC
VCA0752trxC7	CTACACAATCGCTCAAGACGTGACTTCTCTCTTTATTTTGGC
VCA0752trxC8	CTAATTCCCATGTCAGCCGTAACCAAGCGCTGACTAAATAA
VCA0752trxC6	TACGTAGAATGTATCAGACTACGTGCCAAAAGCCAAACAC
VC0281ldclcada5	CTATTATTTAAACTCTTTCCAACGGTGTACCGAAAAAAG
VC0281ldclcada7	CTACACAATCGCTCAAGACGTGTTGGACATCTCCAAGGCGAA
VC0281ldclcada8	CTAATTCCCATGTCAGCCGTGCCAGCTTTACCCATAAAG

VC0281ldclcada6	TACGTAGAATGTATCAGACTCCCTCGCCACTCGCACCCAA
VC1315-165	CTATTATTTAAACTCTTTCCTTTATGTCACACACCGCGAC
VC1315-167	CTACACAATCGCTCAAGACGTGAACGTTTCCTTAATGGCCGA
VC1315-168	CTAATTCCCATGTCAGCCGTGCGATGTTAGGTGAGCTTAG
VC1315-166	TACGTAGAATGTATCAGACTACTAATGAGGGGCATGTTTAT
cpxPAR5	CTATTATTTAAACTCTTTCGTTGAGGATCAAAAAGCAGC
cpxPAR7	CTACACAATCGCTCAAGACGTGCAAAAACACGCTAGTCAATAA
cpxAR8	CTAATTCCCATGTCAGCCGTAGCGCTTAACGCAGTAACTC
cpxAR6bis	TACGTAGAATGTATCAGACTCGCTCAGTGGCCTATCTT
VCA0184capB5	CTATTATTTAAACTCTTTCCTTTTCGCTTTTCCACTCGG
VCA0184capB7	CTACACAATCGCTCAAGACGTGAATAAATATCCTAAAAACATTTTTTAAC
VCA0184capB8	CTAATTCCCATGTCAGCCGTCTGAAAGCATCAAAGTTCTGTAA
VCA0184capB6	TACGTAGAATGTATCAGACTGCGACGCCCATGCAGGCTAT